Cerebral Cortex June 2009;19:1273–1293
doi:10.1093/cercor/bhn167
Advance Access publication September 26, 2008

Molecular Regulation of DNA Damage-Induced Apoptosis in Neurons of Cerebral Cortex

Lee J. Martin[1,2], Zhiping Liu[1], Jacqueline Pipino[1], Barry Chestnut[1] and Melissa A. Landek[1]

[1]Departments of Pathology, Division of Neuropathology and [2]Neuroscience, Johns Hopkins University School of Medicine, Baltimore, MD, USA

Cerebral cortical neuron degeneration occurs in brain disorders manifesting throughout life, but the mechanisms are understood poorly. We used cultured embryonic mouse cortical neurons and an in vivo mouse model to study mechanisms of DNA damaged-induced apoptosis in immature and differentiated neurons. p53 drives apoptosis of immature and differentiated cortical neurons through its rapid and prominent activation stimulated by DNA strand breaks induced by topoisomerase-I and -II inhibition. Blocking p53-DNA transactivation with α-pifithrin protects immature neurons; blocking p53-mitochondrial functions with μ-pifithrin protects differentiated neurons. Mitochondrial death proteins are upregulated in apoptotic immature and differentiated neurons and have nonredundant proapoptotic functions; Bak is more dominant than Bax in differentiated neurons. p53 phosphorylation is mediated by ataxia telangiectasia mutated (ATM) kinase. ATM inactivation is antiapoptotic, particularly in differentiated neurons, whereas inhibition of c-Abl protects immature neurons but not differentiated neurons. Cell death protein expression patterns in mouse forebrain are mostly similar to cultured neurons. DNA damage induces prominent p53 activation and apoptosis in cerebral cortex in vivo. Thus, DNA strand breaks in cortical neurons induce rapid p53-mediated apoptosis through actions of upstream ATM and c-Abl kinases and downstream mitochondrial death proteins. This molecular network operates through variations depending on neuron maturity.

Keywords: Alzheimer's disease, ATM, neonatal brain injury, p53, Parkinson's disease, stroke

Introduction

Degeneration of neurons in the cerebral cortex occurs in many human disorders manifesting acutely or chronically throughout life and causes or contributes to mental retardation, memory decline, dementia, and other functional impairments. In newborns and adults, the cerebral cortex is a major site of neurodegeneration after hypoxia-ischemia, stroke, and trauma (Martin et al. 1998; Zhang et al. 2005; Martin 2008). Cerebral cortical neuron loss occurs in Alzheimer's disease (AD), Parkinson's disease (PD), amyotrophic lateral sclerosis (ALS), Huntington's disease (HD), acquired immunodeficiency syndrome, and neurodevelopmental disorders (Hedreen et al. 1991; Gomez-Isla et al. 1997; Martin 2001; Johnston 2004; Martin et al. 2005; McArthur et al. 2005). The degeneration of neocortical neurons in AD is regionally specific (Gomez-Isla et al. 1997) and might be instigated by Aβ protein toxicity and synapse loss (Sze et al. 1997; Zhang et al. 2002). Loss of pyramidal neurons in the pre-supplementary motor cortex is found in PD (MacDonald and Halliday 2002). Upper motor neurons are cortical neurons; substantial loss of the pyramidal Betz cells occurs in ALS (Nihei et al. 1993; Shaikh and Martin 2002). In HD, neurons in layer 6 of frontal cortex degenerate (Hedreen et al. 1991). The protection of neocortical neurons against degeneration is critical because postnatal regeneration of these neurons in primates through neurogenesis is very limited (Rakic 2002; Breunig et al. 2007). It is therefore necessary to identify the signal transduction networks and specific molecules that mediate death of cerebrocortical neurons because these molecules can become specific targets for the discovery of drugs with potential to block neurodegeneration in many human disorders occurring during development and adulthood.

Apoptosis, a form of programmed cell death, driven by the tumor suppressor p53 is involved in the degeneration of cerebral cortical neurons in a variety of cell and animal models of neuronal death and in some human neurological disorders (Morrison et al. 2003; Martin et al. 2005; Zhang et al. 2005; Northington et al. 2007). During neurodevelopment, telencephalic neural precursor cells with genotoxic stress undergo apoptosis requiring p53 (D'Sa-Eipper et al. 2001). Cortical neuron degeneration occurring after hypoxia-ischemia, stroke, and trauma has a considerable apoptotic component (Hou and MacManus 2002; Zhang et al. 2005); furthermore, in human newborns with hypoxic-ischemic insults due to complications during parturition, neocortical neuron death is associated with oxidative stress and p53 activation (Martin 2008). In adult postmortem human brain, p53 is found in subsets of neocortical and hippocampal neurons in AD (De la Monte et al. 1997; Martin et al. 2005) and in motor cortical neurons in ALS (Martin 2000). p53 and the proapoptotic Bcl-2 family member Bax can mediate toxicity of Aβ to cultured human primary cortical neurons (Zhang et al. 2002), possibly by direct Aβ fibril activation of the p53 promoter (Ohyagi et al. 2005). Part of the activation sequence for p53-mediated apoptosis in cells is the accumulation of DNA damage (Jeffers et al. 2003).

DNA damage has been implicated in the mechanisms of neurodegeneration in age-related disease, cerebral ischemia, and brain trauma. For example, DNA single-strand breaks (SSBs) in neocortex of people with AD are increased 2-fold compared with control subjects (Mullaart et al. 1990), and many cortical neurons in cases of AD show DNA-SSBs and DNA double-strand breaks (DSBs) in situ (Adamec et al. 1999). The neurotoxicity of Aβ in cultured human cortical neurons involves DNA damage triggered by reactive oxygen species (Zhang et al. 2002). Aβ might also exert effects in the AD brain by triggering DNA synthesis in forebrain neurons (Yang et al. 2001). After focal ischemia, DNA-SSBs accumulate very quickly, within 15 min, in cerebral cortex at levels 20-fold higher than baseline (Huang

et al. 2000). These DNA lesions could contribute to delayed neuronal death (Chen et al. 1997) involving DNA synthesis prior to cell death and mitotic catastrophe (Kuan et al. 2004). Similarly, neurons accumulate DNA-SSBs after cortical trauma (Clark et al. 2001). In the developing brain, migrating newborn neurons can sustain oxidative DNA damage and, if not repaired, undergo apoptosis (Narasimhaiah et al. 2005).

Nevertheless, the role of DNA damage as a definitive upstream initiator of postmitotic neuron degeneration or a consequence of the degeneration is vague. In this study we examined the mechanisms of DNA damage-triggered apoptosis of cortical neurons in a cell culture model with confirmed DNA strand breaks and developed a new mouse model of topoisomerase poison-induced apoptosis of cortical neurons. Exposure of neurons to topoiosmerase inhibitors, such as camptothecin (CPT) or etoposide (ETOP), is described frequently as a DNA-damaging stimulus (Park et al. 1998; Keramaris et al. 2000). It is believed, although hitherto unconfirmed, that CPT and ETOP trigger apoptosis in neurons through DNA damage (Endokido et al. 1996; Morris and Geller 1996; Park et al. 1998), but the mechanisms of CPT and ETOP toxicity and cell death in neurons have not been identified clearly, and comparisons in cell death signaling pathways in immature and well-differentiated neurons have not been studied fully (Lesuisse and Martin 2002a, 2002b). We tested the hypotheses, using a combination of gene-disrupted mice and small-molecule drugs, that cerebral cortical neurons at different stages of differentiation have different propensities for DNA damage accumulation and utilize different upstream and downstream molecular signaling pathways in the mediation of cell death in response to DNA damage. This work reveals that the therapeutic protection of neurons in the cerebral cortex of the immature and mature brain could be based on different key molecular targets.

Materials and Methods

Murine Cortical Neuron Culture

To study the effects of DNA damage in postmitotic cells we used primarily a neuronal cell culture model. This approach has many advantages. An essentially pure neuron system is studied without appreciable contamination of cycling cells, such as glia. Also, neurons from the same source can be maintained and differentiated identically over long-term to examine cell death signaling mechanisms in immature cortical neurons or mature, synaptically integrated cortical neurons (Lesuisse and Martin 2002a). The immature and differentiated states of these neurons have been defined previously based on morphology, ultrastructure, and the levels of synaptic and cytoskeletal proteins, glutamate receptors, and metabolic proteins (Lesuisse and Martin 2002a). Furthermore, embryonic cortical neurons can be harvested from mice with targeted gene deletions to identify specific molecules that regulate apoptosis. Timed-pregnant wild-type mice (C57BL/6 strain, The Jackson Laboratory, Bar Harbor, ME) and mice with targeted gene disruptions of *p53*, *bax*, *bak*, or *ATM* (ataxia telangiectasia mutated) (The Jackson Laboratory) were used. Mice with homozygous null deletion of *p53* (B6.129S2-Trp53^{tm1Tyj}; stock number 002101) or *bak* (B6.129-Bak1^{tm1Thsn}; stock number 004183) or with heterozygous null deletion of *bax* (B6.129X1-Bax^{tm1Sjk}; stock number 002994) or *ATM* (129S6/SvEvTac-Atm^{tm1Awb}; stock number 002753) were purchased as breeder pairs to establish colonies of these mice for the generation of primary embryonic cortical neuron cultures. Animal care was provided in accordance with the National Institutes of Health Guide for the Care and Use of Laboratory Animals.

Mouse cortical neuron cultures were prepared as described previously (Lesuisse and Martin 2002a, 2002b). The Animal Care and Use Committee of the Johns Hopkins University School of Medicine approved the animal protocol. Deeply anesthetized (isoflurane: oxygen:nitrous oxide, 1:33:66) pregnant dams underwent cesarean section at 15–16 days gestation for harvesting of mouse embryos. Under a surgical microscope, the brains were dissected from the embryos and the cerebral cortices were isolated carefully and stripped of membranes. The cortices were dissociated by treatment (20 min at 37 °C) with 0.25% trypsin (Invitrogen, Carlsbad, CA) followed by triturating with a fire-polished Pasteur pipette. Cortical tissue was pooled from wild-type, $p53^{-/-}$, and $bak^{-/-}$ null embryos for their respective experiments. For homozygous matings ~16 pregnant mice were used for each genotype. Cortical tissues from *bax* and *ATM* gene deficient mouse embryos were not pooled because they were derived by mating heterozygous mice (e.g., embryos could be $bax^{+/+}$, $bax^{+/-}$, or $bax^{-/-}$). For heterozygous matings ~18 pregnant mice were used. Cortical tissue (both hemispheres) from each of these embryos was digested and plated individually while each embryo was genotyped by PCR (according to the protocol and designated primers from The Jackson Laboratory). Cells (~10^6) were plated onto 35 mm tissue culture dishes coated with 33 μg/ml poly-D-Lysine (Sigma, St Louis, MO) and human fibronectin (Sigma) or onto poly-D-Lysine and laminin coated 12 mm glass coverslips (BD Biosciences, Bedford, MA). The cells were plated in Neurobasal medium (Invitrogen) supplemented with B27 (Invitrogen), 25 μM β-mercaptoethanol (Invitrogen) and streptomycin/penicillin (Invitrogen). Three days after plating, 50% of the medium was changed and subsequently changed every 5 days. This cell culture is nearly neuron-pure because glial contamination of the cell culture is very low (Lesuisse and Martin 2002a). Nevertheless, the cultures prepared in this series of experiments were screened for glial contamination and found to be low as well (<3% oligodendrocytes, <2% astrocytes, <1% microglia), consistent with the inability of serum-free/low glutamine media to support glial cells. Most published in vitro studies of mechanisms of neuronal apoptosis triggered presumably by DNA damage and mediated by p53 have used cultures of primary embryonic or newborn neurons at 2–4 days in vitro (DIV) (Xiang et al. 1998; Keramaris et al. 2003). DIV2–DIV4 neurons are very immature and undifferentiated neurons with very few established synapses which emerge typically at about DIV5 but do not become robust until about DIV10, and then synaptic levels achieve maturity at about DIV15 (Lesuisse and Martin 2002a). In this study we compared apoptotic responses of immature and undifferentiated DIV5 neurons to more mature, highly differentiated DIV25 neurons. For every experiment that was done at different in vitro ages, the neurons in the different differentiation groups were prepared from the same original batches of dissociated cerebral cortices, so that appropriate comparisons could be made (Lesuisse and Martin 2002b). Each experimental data set reported was done at least in triplicate.

Topoisomerase Poison-Induced Cortical Neuron Death in Culture

To study the molecular regulation of cell death in cortical neurons, DNA topoisomerases were inhibited with CPT or ETOP. These 2 poisons were used because they cause DNA damage through different mechanisms (Nitiss and Wang 1996). CPT and ETOP inhibit DNA topoisomerase-I (Topo-I) and DNA topoisomerase-II (Topo-II), respectively (Nitiss and Wang, 1996). Topo-I and Topo-II are nuclear enzymes that modify DNA topology. Topo-I catalyzes DNA single-strand cleavage and reunion of the phosphodiester backbone to allow relaxation of supercoiling in response to a torsional stress generated by replication proteins at replication forks during DNA synthesis or transcriptional proteins during RNA synthesis. Topo-II is a DNA gyrase that cuts simultaneously both strands of the DNA helix, allowing another DNA duplex to pass through the break, followed by religation. CPT and ETOP poisoning of non-neural cells is believed to involve stabilization of Topo-I–DNA complexes or Topo-II–DNA complexes, respectively, and the trapping these enzymes in an intermediate state to disallow religation of the DNA backbone and thus causing the formation of DNA strand breaks (Nitiss and Wang 1996; Nieves-Neira and Pommier 1999). Topo-I is the only know target of CPT, whereas Topo-II is the only known target of ETOP (Bendixen et al. 1990). In cycling cells, CPT and ETOP are thought to be S-phase–specific

antineoplastic agents. CPT induces initially the formation of DNA-SSBs, whereas ETOP induces DNA-DSBs (Nitiss and Wang 1996). CPT can also cause premature termination of transcription and depletion of cellular Topo-I in non-neural cells through its ubiquitination and proteasomal degradation (Bendixen et al. 1990; Nieves-Neira et al. 1999). Their mechanisms of action in postmitotic cells are not as well characterized as in cycling cells. The actions of topoisomerase drugs in postmitotic neural cells could be different from those occurring in cycling cells as illustrated by the different actions of taxol in neuronal cells and non-neuronal cells (Figueroa-Masot et al. 2001). CPT induces apoptosis in immature mixed neuron-astrocyte cultures (Morris and Geller 1996) and in relatively pure immature neuron cultures (Lesuisse and Martin 2002b). ETOP induces apoptosis in cultured embryonic rat brain neurons (Nakajima et al. 1994) and mouse postnatal day 15–16 cerebellar neurons (Endokido et al. 1996). Thus, their S-phase–specific mechanisms of action in postmitotic cells can be questioned or the immature neuronal cultures used are not postmitotic. CPT (Sigma) was dissolved in double-distilled water supplemented with sodium hydroxide and heated at 55 °C for 30 min to dissolve completely the drug at a final concentration of 50 mM. ETOP (Sigma) was dissolved in 4% methyl-β-cyclodextrin (Sigma) in PBS. CPT and ETOP were further diluted in Neurobasal medium. Depending on the particular experimental paradigm, at DIV5 or DIV25, mouse cortical neurons were treated with varying concentrations of CPT or ETOP at 1, 10, or 100 μM for 1, 2, or 4 h or for 4, 8, 15, or 24 h. Low-dose experiments with 0.5 μM CPT or ETOP were conducted over 24, 48, and 72 h.

Antiapoptotic Small-Molecule Drug Screening in Cultured Cerebral Cortical Neurons

Pharmacological manipulations can be done on cultured neurons without major delivery and bioavailability concerns, except solubility and cell permeability of drug. Several compounds were used to examine mechanisms of neuronal cell death and to test for neuroprotective actions, including inhibitors of caspase-3, p53, Bax channel, the voltage-dependent anion channel (VDAC) that is a major component of the mitochondrial permeability transition pore (Bernardi et al. 2006), ATM, and c-Abl (Table 1). The justification for using each of these drugs is given in the results. The drugs were prepared as 10 mM stock solutions in dimethyl sulfoxide or water and then diluted in media and used at final concentrations of 1–100 μM in cultures. The concentrations used were based on published literature on the application of these drugs in cell systems and on empirical titration experiments done on neurons (data not shown). Cells were pretreated for 2 h with drug or vehicle before exposure to CPT or ETOP.

Cell Survival and Cell Death Analysis in Cortical Neuron Cultures

For quantification of living neuron densities, cells were viewed under phase contrast optics using a Nikon Eclipse TS100 microscope (40× objective) equipped with an Infinity camera to capture digital images from 6 nonoverlapping microscopic fields. For quantification of neuronal apoptosis, fixed cultures were stained with a nuclear dye (Hoechst 33258), digital images were captured from 6 nonoverlapping microscopic fields, and apoptotic nuclei were counted as before (Lesuisse and Martin 2002b).

Western Blot and Immunoprecipitation of Cultured Cortical Neuron Proteins

Cell lysates were made from control and CPT-treated neurons for Western blot analyses. DIV5 and DIV25 cortical neuron cultures (3 different platings) were treated with 10 μM CPT and cells were harvested 1, 2, 4, 8, 15, and 24 h later. Cortical neuron cultures were lysed in TNE buffer (10 mM Tris–HCl, pH 7.4, 150 mM NaCl, and 5 mM ethylenediaminetetraacetic acid) containing protease inhibitors (1 mM phenylmethanesulphonylfluoride (PMSF), 10 μg/ml leupeptin, and 10 μg/ml pepstatin A) and detergents (2% sodium dodecyl sulfate [SDS], 1% deoxycholate, and 1% NP-40), and sonicated for 15 s. Because most of the primary antibodies used were generated against human proteins, samples of human cerebral cortex were used as positive controls in some western blot experiments. The human brain autopsy tissue was obtained from the Human Brain Resource Center at Johns Hopkins as described previously (Martin, 2000). Protein concentrations of each homogenate were determined by protein assay (Pierce, Rockford, IL). Homogenates were diluted further in Laemmli sample buffer.

Protein (20 μg) from neuronal cultures were resolved on gradient SDS polyacrylamide gels (4–20%) and transferred to nitrocellulose filter membranes by electroblotting. Nitrocellulose membranes were blocked in 5% (w/v) nonfat dry milk in phosphate-buffered saline (PBS). After overnight incubation with the primary antibodies (Table 2) in PBS supplemented with 5% nonfat dry milk and 0.05% (v/v) Tween-20, membranes were rinsed and then incubated with peroxidase-conjugated secondary antibody. Immunoreactive proteins were visualized on x-ray film using enhanced chemiluminescence (Pierce).

Immunoprecipitation and western blot analysis of cell lysates from CPT-treated and control neurons were used to identify p53 and c-Abl as targets of ATM/ATM-Rad3–related kinase (ATR). Briefly, 100 μg of total lysate protein was immunoprecipitated using 5 μg of mouse monoclonal antibody to p53 or c-Abl (Table 1, Santa Cruz, Biotechnology, Santa Cruz, CA). After immunocapture with immobilized protein A/G

Table 1
Pharmacological agents used to manipulate apoptosis in cerebral cortical neurons

Agent	Class	Action	Source
CH95	Small molecule, nonpeptide	Caspase-3 inhibitor	A.G. Scientific, San Diego, CA
Cyclic-pifithrin-α	Small molecule, nonpeptide	Inhibitor of p53 transactivation	Calbiochem, Gibbstown, NJ
Pifithrin-μ	Small molecule, nonpeptide	Inhibitor of p53 interaction with Bcl-X_L/Bcl-2	Calbiochem
Actinomycin D	Small molecule	RNA synthesis inhibitor	Sigma
Cycloheximide	Small molecule	Protein synthesis inhibitor	Calbiochem
Bax-channel blocker	Small molecule, nonpeptide	Inhibitor of Bax-channel activity	Calbiochem
Bax-inhibiting peptide	Pentapeptide	Inhibitor of Bax conformational change and mitochondrial translocation	Calbiochem
Bax-inhibiting peptide, negative control	Pentapeptide	Nonfunctional mutated analog of Bax-inhibiting peptide	Calbiochem
Bak-BH3	Fusion peptide consisting of death-promoting Bak-BH3 domain and Antennapedia internalization sequence	Binds and inactivates Bcl-xL	Calbiochem
Bak-BH3, negative control	Fusion peptide consisting of the Antennapedia internalization sequence and a mutated Bak-BH3 sequence	Nonfunctional	Calbiochem
Bcl-xL-$BH4_{4-23}$	Fusion peptide consisting of BH4 domain of Bcl-X_L linked to the HIV-TAT carrier peptide	Binds and inhibits the VDAC	Calbiochem
Ku-55933	Small molecule, nonpeptide	Specific and potent inhibitor of ATM	Calbiochem
Caffeine	Small molecule, nonpeptide	Inhibitor of ATM	Sigma
STI571 (CGP57148B)	Small molecule, nonpeptide	Inhibitor of c-Abl	Novartis, Basel, Switzerland

(Pierce) the samples were subjected to SDS-polyacrylamide gel electrophoresis and electroelution onto nitrocellulose membrane for the detection of phospho-ATM/ATR substrate proteins (Table 2, Cell Signaling Technology, Danvers, MA). The efficiency of immunocapture was estimated by immunoblotting to be ~55% of total p53 or c-Abl.

Immunocytochemistry

Immunofluorescence was used to visualize cleaved caspase-3 and phospho-p53 in control and CPT-treated cortical neurons. Cells were fixed in 4% paraformaldehyde/4% sucrose in PBS (4 °C, 20 min) and then with methanol (4 °C, 10 min), and then permeabilized in 0.2% Triton X-100, 10% normal goat serum (NGS) in PBS (4 °C, 10 min), incubated overnight at 4 °C in 10% NGS in PBS with primary antibody to cleaved caspase-3 (D175, Cell Signaling, Technology) or phospho-p53 (Cell Signaling). Antibody binding was visualized with Alexa-488- or Cascade blue-conjugated goat anti-rabbit (Invitrogen) diluted at 1:600 in PBS. p53 immunostained cells were also dual-labeled with an antibody to manganese superoxide dismutase (Assay Design, An Arbor, MI) as a mitochondrial marker. Immunofluorescence preparations with viewed with a Nikon TS100 microscope and digital images were captured with a Nikon Infinity CCD camera or they were viewed using a Zeiss LSM confocal microscope.

Caspase-3 Activity Assay

Cortical neurons were lysed in cell lysis buffer, microcentrifuged (10 000 × *g*), and supernatants were evaluated for the activity of caspases that recognize the DEVD sequence using a colorimetric assay kit based on the detection of *p*-nitroaniline after cleavage from DEVD

Table 2
Antibodies used for cell death molecule detection in cerebral cortical neurons

Antibody	Source	Catalog no.	Origin clone/isotype	Antigen	Controls
Cleaved caspase-3	Cell Signaling Technology	9661	Rabbit polyclonal IgG	Human caspase-3 cleavage site peptide (aa 165–175)	Neurons with (+) and without (−) cell death
Topoisomerase I (Topo-I)	Santa Cruz Biotechnology	sc-5342	Goat polyclonal IgG	Human Topo-I c-terminus	HeLa cell nuclear extracts (+); blocking peptide (−)
Phospho-Ser15-p53 (mouse Ser18-p53)	Cell Signaling Technology	9284	Rabbit polyclonal IgG	Phospho-Ser^{15} peptide (aa 9–22) of human p53	Neurons with (+) and without (−) cell death; sample treatment with λ-phosphatase (−)
Phospho-Ser15-p53	R&D Systems, Minneapolis, MN	AF1043	Rabbit polyclonal IgG	Phospho-Ser^{15} peptide of human p53	Neurons with (+) and without (−) cell death; sample treatment with λ-phosphatase (−)
p53, pan	Beohringer Mannheim (Roche), Indianapolis, IN	1810928	Sheep polyclonal IgG	Human recombinant p53	Recombinant p53 (+); p53-null mouse tissues/neurons (−)
p53, pan	Santa Cruz Biotechnology	sc-99	Pab240 mouse monoclonal IgG	aa 156–214 of human p53	Recombinant p53 (+); p53-null mouse tissues/neurons (-)
Bax	Upstate Biotechnology, Lake Placid, NY	06-499	Rabbit polyclonal IgG	aa 1–21 of human Bax	Bax-null mouse tissues/neurons (−)
Bak	Upstate Biotechnology	06-536	Rabbit polyclonal IgG	aa 23–37 of human Bak	Bak-null mouse tissues/neurons (−)
PUMA	Upstate Biotechnology	07-669	Rabbit polyclonal IgG	aa 2–16 of human Puma	Recombinant protein (+); Puma null tissues (−)
Noxa	Imgenex, San Diego, CA	IMG-451	Rabbit polyclonal IgG	aa 51–66 and 75–90 of mouse Noxa	Recombinant protein (+); nonapoptotic neurons (−)
ATM/ATR phospho-substrate	Cell Signaling Technology	2851	Rabbit polyclonal IgG	Synthetic phospho-Ser/Thr peptides (L-S/T-Q motif)	sample treatment with λ-phosphatase (−); irradiated HeLa cells (+)
PhosphoSer1981 ATM	Cell Signaling Technology	4526	10H11.E12 mouse monoclonal IgG	aa residues surrounding phospho-Ser1981 of human ATM	sample treatment with λ-phosphatase (−); irradiated HeLa cells (+)
ATM, pan	GeneTex, San Antonio, TX	GTX70103	2C1 mouse monoclonal IgG	Recombinant human ATM	ATM-null mouse tissues/neurons (-); irradiated HeLa cells (+)
PhosphoTyr245-cAbl	Cell Signaling Technology	2861	Rabbit polyclonal IgG	aa residues surrounding phospho-Tyr245 of human cAbl	Sample treatment with λ-phosphatase (−); RAW cells (+)
c-Abl	Santa Cruz Biotechnology	sc-23	24-11 mouse monoclonal IgG	c-terminal domain of human c-Abl	RAW cells (+)
Phospho-Ser-3 coflin	Chemicon	AB3831	Rabbit polyclonal IgG	aa residues surrounding phospho-Ser3 of human coflin	Sample treatment with λ-phosphatase (−); human cells/tissue (+)

Figure 1. CPT causes in cortical neurons inactivation of Topo-I, accumulation of DNA-SSBs and -DSBs in neurons, and induces caspase 3–dependent apoptosis. (*A*) Hoechst 33258 staining of DIV5 neuron nuclei in vehicle control and 10 μM CPT-treated cells. There are few apoptotic neurons (nuclei that are bright white and condensed into single or multiple round aggregates) in controls, whereas most neurons are apoptotic after 24 h of CPT exposure. Scale bar = 7 μm. Graph shows that the amount of apoptosis is dose-dependent in DIV5 (immature) and DIV25 (mature-differentiated) neurons. Values are mean ± SD based on at least 6 images of Hoechst-stained cells per group. Results were replicated in 3 different cell culture experiments. Symbols denote: significantly greater $^{*}P < 0.01$, $^{**}P < 0.001$, and $^{+}P < 0.005$ versus vehicle; significantly lower $^{\#}P < 0.05$ versus concentration-matched DIV5 neurons. (*B*) Western blots showing rapid and dramatic loss of Topo-I protein with 10 μM CPT treatment for 4 through 24 h in DIV5 and DIV25 neurons. Ponceau S staining of nitrocellulose membrane shows protein loading. (*C*) Plasmid DNA-based Topo-I activity assay on DIV5 neuron extracts showing decreased formation of DNA topoisomers (relaxed DNA) from supercoiled DNA at 4 h of 10 μM CPT exposure. Results were confirmed using 2 amounts of total protein (2.5 and 5 μg). (*D*) Cleaved caspase-3 immunoreactivity (Alexa-488 green labeling) accumulates robustly by 8 h of CPT treatment in most DIV5 and DIV25 cortical neurons. Scale bar = 10 μm. Only a few isolated neurons are positive for cleaved caspase-3 in vehicle control cultures (upper left inset, green dots, see arrow). Inset scale bar = 80 μm. (*E*) Capase-3 activity, determined by biochemical colorimetric assay, is increased in DIV5 and DIV25 cortical neurons in a time-related manner after 10 μM CPT exposure. Values (in units × 10^{-1}) are mean ± SD ($n = 3$ different cultures of 6 pooled 35 mm wells per data point). Significantly greater $^{*}P < 0.05$, $^{**}P < 0.001$ and $^{+}P < 0.01$ versus vehicle; significantly lower $^{\#}P < 0.01$ versus timed-matched DIV5 neurons. (*F*) Inhibition of apoptosis induced by 10 μM CPT in both DIV5 and DIV25 neurons with the small-molecule nonpeptide caspase-3 inhibitor CH95. Values are mean ± SD based on at least 6 images of Hoechst-stained cells per group and were replicated in 3 different culture experiments. Symbols denote: significantly greater $^{*}P < 0.01$, $^{**}P < 0.001$ and $^{+}P < 0.005$ versus vehicle; significantly lower $^{\#}P < 0.05$ versus CPT treatment alone. (*G*) Alkaline and neutral comet assays show accumulation of DNA-SSBs and DNA-DSBs in immature DIV5 neurons and mature DIV25 neurons after 4 h exposure to 10 μM CPT. DNA is stained with SYBR Green. Few control neurons have comet tails. Most CPT-treated neurons have comet tails indicating DNA-SSBs or -DSBs. (*H*) Quantification of the percentage of DIV5 and DIV25 neurons with DNA-SSBs after 4 h exposure to 10 μM or 50 μM CPT as determined by alkaline comet assay. Values are mean ± SD based on at least 10 images per group and were replicated in 2 different culture experiments and comet assays. Symbols denote: significantly greater $^{*}P < 0.005$, $^{**}P < 0.001$, and $^{+}P < 0.01$ versus vehicle; significantly lower $^{\#}P < 0.01$ versus concentration-matched DIV5 neurons. (*I*) Quantification of the percentage of DIV5 and DIV25 neurons with DNA-DSBs after 4 h exposure to 10 or 50 μM CPT as determine by neutral comet assay. Values are mean ± SD derived from at least 10 images per group and were replicated in 2 different culture experiments and comet assays. Symbols denote: significantly greater $^{*}P < 0.001$ than control.

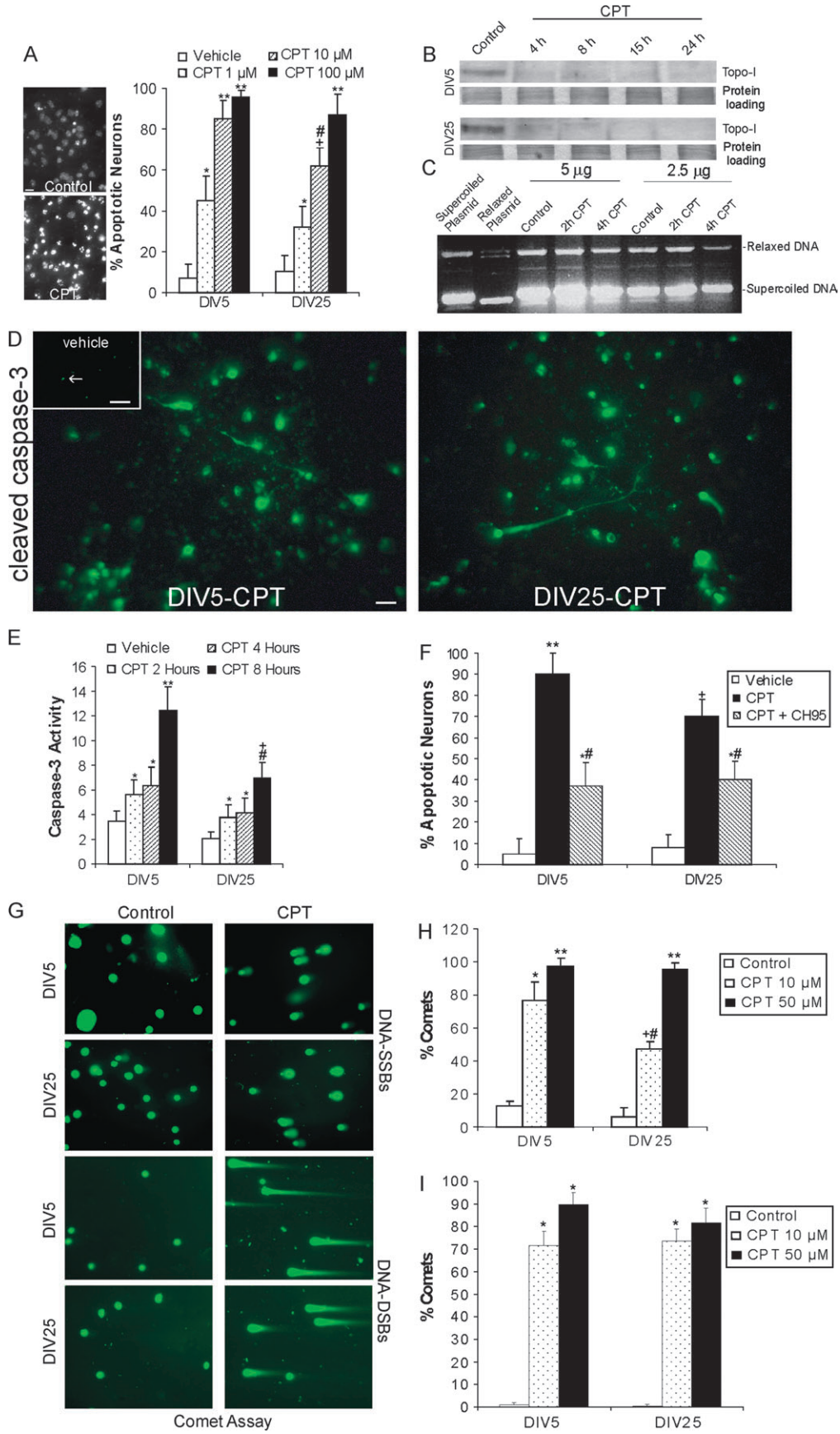
A
Vehicle
CPT 1 μM
CPT 10 μM
CPT 100 μM
Control
CPT
% Apoptotic Neurons
DIV5
DIV25
B
CPT
Control
4 h
8 h
15 h
24 h
DIV5
DIV25
Topo-I
Protein loading
C
5 μg
2.5 μg
Supercoiled Plasmid
Relaxed Plasmid
Control
2h CPT
4h CPT
Relaxed DNA
Supercoiled DNA
D
cleaved caspase-3
vehicle
DIV5-CPT
DIV25-CPT
E
Vehicle
CPT 4 Hours
CPT 2 Hours
CPT 8 Hours
Caspase-3 Activity
DIV5
DIV25
F
Vehicle
CPT
CPT + CH95
% Apoptotic Neurons
DIV5
DIV25
G
Control
CPT
DIV5
DIV25
DNA-SSBs
DNA-DSBs
Comet Assay
H
Control
CPT 10 μM
CPT 50 μM
% Comets
DIV5
DIV25
I
Control
CPT 10 μM
CPT 50 μM
% Comets
DIV5
DIV25

(Chemicon, Temecula, CA). Absorbance was read spectrophotometrically at 405 nm. Human recombinant active caspase-3 (Chemicon) was used as a positive control. Treatment of samples with caspase-3 inhibitor (Ac-DEVD-CHO) was the negative control.

Topoisomerase I Activity Assay

Crude lysates of cortical neurons were evaluated for Topo-I activity using an assay kit that is highly specific for Topo-I activity with no contribution of Topo-II (TopoGEN, Port Orange, FL). This assay is based on the ability of Topo-I to catalyze ATP-independent relaxation of negatively supercoiled plasmid DNA. Relaxation assays were carried out with 2.5–5 μg cortical neuron lysate protein in a final volume of 25 μL in Topo-I reaction buffer (100 mM Tris-Cl, pH 7.9, 1.5 M NaCl, 1% bovine serum albumin, 1 mM spermidine, 50% glycerol). Supercoiled plasmid DNA (0.25 μg) was used as substrate. Reactions were terminated with 5 μL (per 20 μL reaction volume) of stop buffer (5% sarkosyl, 0.0025% bromophenol blue, 25% glycerol). Reaction products were analyzed on 1% native agarose gels.

Single-Cell Gel Electrophoresis (Comet) Assay for DNA Damage

There are many different forms of DNA damage (Lindahl 1993), so we used the comet assay to profile, using specific pH conditions, DNA-SSBs and DNA-DSBs directly in mouse cortical neurons. This assay is exquisitely sensitive, detecting one strand-break per 2×10^{10} Daltons of DNA (Kindzelskii and Petty 1999), and quantitative for measuring early damage to genomic DNA of eukaryotic cells on a single-cell basis (Tice et al. 2000). We found previously that oxidative stress by hydrogen peroxide, nitric oxide donors, and peroxynitrite all induce DNA-SSBs in primary motor neurons (Martin and Liu 2002). Cortical neurons at DIV5 and DIV25 were exposed to CPT, ETOP, or vehicle and then collected at 4 h for DNA-SSB and DNA-DSB determinations using alkaline and neutral comet assays, respectively, essentially as described (Martin and Liu 2002) but with some modifications, including the use of CometSlides (Trevigen, Gaithersburg, MD) for embedding of ~1000 neurons per slide and SYBR Green staining of DNA instead of ethidium bromide staining after gel electrophoresis. Slides were viewed (excitation 425–500 nm) with a Zeiss Axiophot epifluorescence and at least 10 images (10–20 nuclei per image)/slide were captured at a magnification of 200×. Two Cometslides were used for each condition. With this excitation wavelength DNA-bound SYBR Green fluoresces green (Fig. 1*G*). In normal neurons the fluorescence is confined mostly to the nucleoid (nucleus after assay) because the DNA is undamaged and supercoiled and cannot migrate far in the electric field. In neurons with DNA damage, the DNA is unwound by the alkali solution for SSB detection, or neutral solution for DSB detection, and the negatively charged DNA fragments are released from the nucleus and migrate toward the anode. The length of DNA extrusion from the nucleoid is proportional to the amount of accumulated DNA-SSBs or DNA-DSBs (Martin and Liu 2002). The percentage of neurons yielding nucleoids with comets relative to the total number of neurons was determined from digital images.

Cell Death Protein Expression in Developing Mouse Brain

As a first step to authenticate our observations made in cell culture as events that occur in brain, we studied the expression of selected cell death proteins in the developing mouse brain. Deeply anesthetized wild-type C57BL/6 mice were killed by decapitation on the day of birth (P0) and at postnatal day 5 (P5), 10 (P10), 15 (P15), and 20 (P20). The fresh forebrains were used to prepare subcellular fractions that were analyzed by Western blotting as described (Martin et al. 2003). In this developmental series, nuclear fractions were used to evaluate expression of phospho-53 and mitochondrial-enriched fractions were used to evaluate Bax, Bak, Noxa, and Puma. The subcellular fractionation method has been validated (Martin et al. 2003). Subcellular fractions of human cerebral cortex gray matter (Martin 2000) were used as positive or negative controls because the primary antibodies were raised against human protein sequences.

Mouse Brain Model of CPT-Induced Neurodegeneration

To further define the relevance of observations in a cell culture model system as events that occur in injured brain, we used CPT in an in vivo setting. C57BL/6 mouse dams with litters were used. The day of delivery was designated as P0. Pups with dams were housed in a laboratory animal suite with an ambient temperature of 23 °C, 12-h light/dark cycle, and ad libitum access to food and water. The Animal Care and Use Committee of the Johns Hopkins University School of Medicine approved the animal protocol. CPT was injected directly into the brain of wild-type and *bak*$^{-/-}$ mouse pups at P5. The CPT was the same stock as that used for cultured neuron experiments. Pups were deeply anesthetized (isofluorane/nitrous oxide/oxygen) and were placed in a neonatal small animal stereotaxic apparatus (Stoelting, Wood Dale, IL). Surgical anesthesia was maintained with isoflurane and nitrous oxide. Body temperature was maintained with external warming. The scalp was cleaned with betadine and 70% isopropyl alcohol prior to making a midsagittal incision. A small burr hole in the skull over the right hemisphere was made with a fine tip dental drill bit. CPT (10 μM, 1 μL total volume) or an equal volume of PBS was injected stereotaxically with a 10-μL Hamilton syringe (Hamilton Company, Reno, NV) into the lateral ventricle. CPT was delivered over 1 min; the needle was left in place for 3 min before it was withdrawn slowly to prevent leakage of drug and cortical trauma. The craniotomy was unsealed, the scalp was sutured, and the pup was returned to the dam.

CPT-treated and vehicle-treated mouse brains were analyzed for biochemical and histological changes indicative of apoptosis. CPT-treated and control mice were killed at 8 h (n=6) or 16 h (n = 6). Brains were removed for western blot analysis of phospho-p53, Bax, and Bak. Another cohort of mice was killed by an overdose of sodium pentobarbital followed by perfusion-fixation with aldehydes at 24 h after injection of CPT (n = 6) or vehicle (n = 6). Brains were harvested, cryoprotected, and cut serially into 40-μm-thick sections using a freezing microtome (American Optical Corporation, Buffalo, NY). To assess effects of CPT in brain, every 10th section was mounted on adhesive-coated glass microscope slides (Fisher, Pittsburgh, PA), dried, dehydrated with alcohols, defatted with xylenes, and stained with cresyl violet to observe apoptotic profiles.

Statistical Analysis

All quantitative data are expressed as mean ± standard deviation. Statistical analysis among groups was performed with one-way analysis of variance (ANOVA) or 2-way ANOVA followed by the Duncan's multiple range test, with $P < 0.05$ considered statistically different.

Results

CPT Causes Inactivation of Topo-I, Accumulation of DNA Strand Breaks, and Caspase 3–Dependent Apoptosis in Cortical Neurons

We determined if embryonic cortical neurons cultured to different stages of differentiation (Lesuisse and Martin 2002a) have different responses to CPT, which is presumed to cause DNA damage in neurons. Cortical neurons at DIV5 (immature and undifferentiated) and DIV25 (mature and differentiated) were treated with 1, 10, or 100 μM CPT or with vehicle and then evaluated for apoptosis after 24 h as gauged by nuclear morphology with Hoechst 33258 staining (Fig. 1*A*). All concentrations of CPT-induced apoptosis in cortical neurons with a similar light microscopic morphology (Fig. 1*A*, left) as described before (Lesuisse and Martin 2002b), and the amount of apoptosis was dose-dependent (Fig. 1*A*, right). At the 10 μM dose, DIV5 neurons were more sensitive than DIV25 neurons, as evidenced by the greater percentage of apoptotic neurons (Fig. 1*A*, right, 2-way ANOVA). Western blotting revealed that differentiated neurons have higher levels of Topo-I, detected at ~120 kDa, than immature neurons and that 10 μM CPT treatment induced rapidly a loss of Topo-I in both DIV5 and DIV25 neurons (Fig. 1*B*). The loss of Topo-I protein seen at 4 h of 10 μM CPT treatment was paralleled by a loss of functional

enzyme activity as seen by decreased formation of relaxed plasmid DNA topoisomers (Fig. 1*C*).

Immunocytochemistry on fixed DIV5 and DIV25 cortical neurons treated with 10 μM CPT revealed numerous neurons immunopositive for cleaved caspase-3, but very few neurons in control cultures displayed immunoreactivity for cleaved caspase-3 (Fig. 1*D*). In keeping with the immunolabeling, both DIV5 and DIV25 neurons treated with 10 μM CPT showed a time-related increase in caspase-3 enzyme activity (Fig. 1*E*). At both stages of differentiation, caspase-3 activity was increased significantly at 2 hof CPT exposure, and 3- to 4-fold increases were observed at 8 h. DIV5 neurons had a greater increase in caspase-3 activity compared with DIV25 neurons (Fig. 1*E*). The effect of increased caspase-3 activity in mediating apoptosis in this system was determined by pretreating neurons with a novel small-molecule non-peptide inhibitor of caspase-3, shown previously to potently and selectively block caspase-3 in vitro and in vivo (Chen et al. 2006). CH95 promoted significant decreases in the amount of neuronal apoptosis, resulting in ~38% and ~42% neuroprotection in both immature and differentiated neurons, respectively (Fig. 1*F*).

It has been assumed that CPT triggers apoptosis in neurons by inducing DNA strand breaks (Park et al. 1998; Stefanis et al. 1999) as in cycling non-neuronal cells (Nieves-Neira and Pommier 1999), but this has not been confirmed in neurons. To understand the upstream mechanism through which CPT triggers apoptosis in immature and mature cortical neurons, we evaluated neurons for the presence of DNA strand breaks using alkaline and neutral comet assays, which detect selectively DNA-SSBs or DNA-DSBs under these conditions, respectively (Martin and Liu 2002). In both DIV5 and DIV25 cortical neurons both DNA-SSBs and -DSBs accumulated significantly with 4 h of CPT exposure (Fig. 1*G-I*). Counts of comet profiles in microgels revealed dose-dependent accumulation of cortical neurons harboring DNA-SSBs (Fig. 1*H*). The accumulation of DNA-DSBs was not CPT-dose-related (Fig. 1*I*). Immature neurons accumulated more DNA-SSBs compared with differentiated neurons after 10 μM CPT treatment (Fig. 1*H*). There was no difference between DIV5 and DIV25 neurons with the 50 μM CPT (Fig. 1*H*), and the accumulation of DNA-DSBs in immature and differentiated neurons was similar (Fig. 1*I*).

p53 Mediates DNA Damage-Induced Apoptosis in Immature and Differentiated Cortical Neurons

The accumulation of DNA damage leads to p53 activation through phosphorylation and subsequent apoptosis in cycling cells (Giaccia and Kastan 1998). We therefore evaluated total cell lysates of CPT-treated cortical neurons at different stages of maturation for the presence of p53 activation as witnessed by its phosphorylation at an N-terminal serine residue (Fig. 2*A*,*B*). This antibody specifically detects human p53 and mouse p53 only when serine-15 or serine-18, respectively, is phosphorylated; serine-15 in human p53 and serine-18 in mouse p53 are homologous with regard to p53 function (Chao et al. 2000). In well-maintained control cultures of mouse cortical neurons at DIV5 and DIV25, the level of active p53 is very low (Fig. 2*A*,*B*). Both DIV5 and DIV25 neurons had markedly higher levels of phospho-p53 compared with age-matched controls after exposure to 10 μM CPT. We evaluated first a 4- to 24-h time course and found the accumulation of phosphorylated p53 already at 4 h of CPT exposure (Fig. 2*A*). DIV5 neurons mounted a sharp ~80-fold increase in p53 phosphorylation with 4 and 8 h exposure to CPT, which then dissipated to a 20-fold increase above control (Fig. 2*A*, right). In DIV25 neurons there was also a high increase (~25-fold) in p53 phosphorylation at 4 h of CPT exposure, but then the level of phosphorylated p53 declined progressively, although remaining significantly above control levels (Fig. 2*A*, right). We then evaluated CPT-treated DIV5 neurons over a 1- to 4-h period (Fig. 2*B*), using lower amounts of protein loading in an effort to detect more subtle gradations in p53 phosphorylation in this more collapsed time course compared with the earlier experiment (Fig. 2*A*). There was a significant increase in p53 phosphorylation at 1 hour of treatment, and then phosphorylation further increased progressively to achieve ~50-fold higher levels above control (Fig. 2*B*, right). These increases in phospho-p53 occurred in the absence of elevations in the overall levels of p53 as detected with pan-p53 antibody (Fig. 2*A*,*B*). This immunoreactive band is known to be p53 because it is absent in $p53^{-/-}$ mouse brain (Martin et al. 2003) and in primary embryonic neuron cultures from these mice (data not shown). Immunocytochemistry on fixed neurons treated with CPT for 4 h showed numerous DIV5 and DIV25 neurons immunoreactive for phospho-p53 (Fig. 2*C*). Cultures under baseline conditions or vehicle treatment had very few neurons immunoreactive for phospho-p53 (Fig. 2*C*, lower left inset), consistent with the low level of phospho-p53 detected in controls by western blotting (Fig. 2A,B). After CPT treatment, DIV25 neurons were different from DIV5 neurons in that they showed cytoplasmic and nuclear phospho-p53 accumulation (Fig. 2*C*, right), but DIV5 neurons primarily had nuclear accumulation of phospho-p53 (Fig. 2*C*, left). Some cytoplasmic p53 immunoreactivity was localized to mitochondria in CPT-treated differentiated DIV25 neurons (Fig. 2*C*, right inset).

To determine if p53 participates causally in the mechanisms of cortical neuron apoptosis and to evaluate possible differential molecular requirements for cell death depending on neuron differentiation, we used genetic and pharmacological manipulations. Cortical neuron cultures were prepared from wild-type and $p53^{-/-}$ mouse embryos, maintained for 5 or 25 days, and treated with 10 μM CPT for 24 h. The apoptotic response of $p53^{-/-}$ DIV5 neurons was blocked nearly completely, whereas the apoptotic response of $p53^{-/-}$ DIV25 neurons was blocked by about 50% (Fig. 2*D*). In another experimental paradigm, wild-type $p53^{+/+}$ cortical neurons were treated with 2 inhibitors of p53 that have different mechanisms of action (Fig. 2*E*): cyclic-α-pifithrin (α-PFT) that blocks reversibly p53-dependent transactivation of p53-dependent responsive genes in non-neuronal cells (Komarov et al. 1999) or μ-PFT that blocks p53 interaction with Bcl-xL and Bcl-2 and inhibits selectively p53 translocation to mitochondria without affecting the transactivation function of p53 at the level of the genome in non-neuronal cells (Strom et al. 2006). In DIV5 $p53^{+/+}$ neurons, the level of apoptosis was reduced from ~87% to 35% of neurons with α-PFT treatment (Fig. 2*E*). μ-PFT was much less effective than α-PFT in reducing the apoptosis in DIV5 $p53^{+/+}$ neurons, although still having significant effect (Fig. 2*E*). Treatment of cortical neurons with α-PFT and μ-PFT did not provide significant antiapoptotic action over α-PFT alone in DIV5 neurons. In contrast, in DIV25 $p53^{+/+}$ neurons μ-PFT was significantly more effective than α-PFT in blocking apoptosis (Fig. 2*E*). As control experiments for drug specificity, treatment experiments with α-PFT and μ-PFT were repeated in

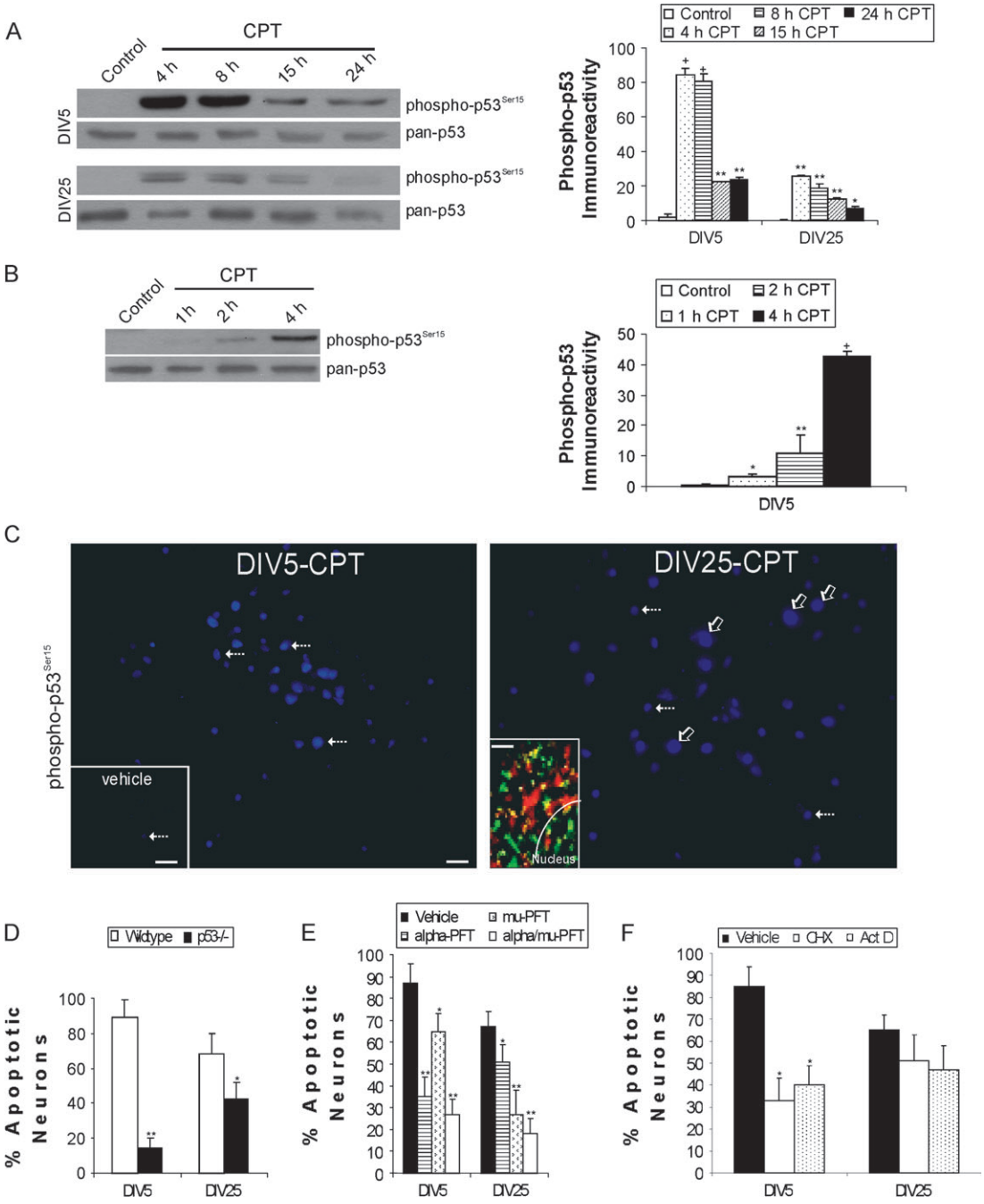

Figure 2. p53 regulates DNA damage-induced apoptosis in immature and mature cortical neurons through partly different mechanisms. (*A*) Western blots showing robust activation of p53 through phosphorylation of serine-15 (detected with phosphorylation state-specific antibody) with 10 μM CPT treatment for 4 through 24 h (h) in DIV5 and DIV25 neurons (10 μg total protein loaded per lane). Total levels of p53 (detected with a phosphorylation state-independent pan antibody) remain stable or decrease over time. Graph shows the optical density measurements of phospho-p53 (in relative OD units) in DIV5 (immature) and DIV25 (mature-differentiated) neurons with 10 μM CPT treatment. Values are mean ± SD ($n = 3$ different cultures of 6 pooled 35 mm wells per data point). Symbols denote: significantly greater $^{+}P < 0.0001$, $^{**}P < 0.001$, and $^{**}P < 0.01$ versus vehicle. (*B*) Western blot showing rapid activation of p53 by phosphorylation of serine-15 (detected with phosphorylation state-specific antibody) with 10 μM CPT treatment for 1 through 4 h in DIV5 neurons (7 μg total protein loaded per lane). Total levels of p53 (detected with a phosphorylation state-independent pan antibody) remain stable over this time course. Graph shows the optical density measurements of phospho-p53 (in relative OD units) in DIV5 neurons with 10 μM CPT treatment. Values are mean ± SD ($n = 3$ different cultures of 6 pooled 35 mm wells per data point). Symbols denote: significantly greater $^{+}P < 0.001$, $^{**}P < 0.01$, and $^{*}P < 0.05$ versus vehicle. (*C*) Phospho-p53 immunoreactivity (cascade blue labeling) is present robustly at 4 h of CPT treatment in many DIV5 and DIV25 cortical neurons. In DIV5 neurons treated with CPT, phospho-p53 immunoreactivity is confined mostly to the nucleus (hatched arrows) in positive cells. In DIV25 neurons treated with CPT, phospho-p53 immunoreactivity is present throughout the cell body (nucleus and cytoplasm) in many neurons (open arrows), but in some neurons in the same microscopic field p53 immunoreactivity is confined to the nucleus (hatched arrows). Note that nuclei with p53 staining (hatched arrows) in DIV5 and DIV25 neurons have similar sizes, whereas the neurons with both cytoplasmic and nuclear labeling in DIV25 cultures are larger because the entire cell body is labeled. Scale bar in DIV5-CPT image = 10 μm (same bar for DIV-25 image). Only a few nuclei are positive for phospho-p53 (blue labeling) in vehicle control cultures (lower left inset, hatched arrow). Vehicle inset scale bar = 80 μm. Immunocytochemical dual labeling (lower left inset in right panel) for phospho-p53 (green) and the mitochondrial marker manganese superoxide dismutase (red) reveals a mitochondrial localization for some p53 (seen as yellow) in CPT-treated DIV25 neurons. The white curved line delineates partially the border between the nucleus and the cytoplasm (inset scale bar = 0.5 μm). (*D*) *p53* gene deletion reduces apoptosis in DIV5 and DIV25 cortical neurons treated with CPT for 24 h. Values are mean ± SD based on at least 6 images of Hoechst-stained neurons per group and were replicated in

p53$^{-/-}$ neuron cultures, no additional neuroprotection was observed over that provided by the null mutations (data not shown).

This experiment suggested that apoptosis in immature and differentiated cortical neurons might have different levels of transcriptional dependence. This suspicion was confirmed by treating wild-type cortical neurons with a low concentration of cycloheximide (1 μg/mL) or actinomycin D (1 μg/mL) prior to CPT exposure. Both agents blocked the apoptosis in DIV5 neurons but not in DIV25 neurons (Fig. 2*F*).

Cell Death Effectors of Apoptosis Downstream of p53 are Regulated Differentially in Immature and Differentiated Cortical Neurons

The mechanisms of cortical neuron apoptosis downstream of p53 activation were analyzed (Fig. 3). We examined by Western blotting mediators of apoptosis in cell lysates of CPT-treated neurons harvested after different times of exposure. Multidomain (Bak and Bax) and BH3-only (Puma and Noxa) members of the Bcl-2 family were measured over a 4-h CPT exposure time course. Bak, detected at ~30 kDa, was increased markedly in CPT-treated cortical neurons, but the temporal patterns were different in DIV5 and DIV25 neurons. In DIV5 neurons there was a modest but significant increase in Bak at 1 h of CPT exposure and then a large ~4-fold spike in Bak levels at 2 h, followed by a diminution in the increase at 4 h (Fig. 3*A*,*B*). In DIV25 neurons baseline control Bak levels were significantly higher (>3-fold) than in control DIV5 neurons, and CPT-treated DIV25 neurons mounted a sustained elevation (~2-fold) in Bak compared with DIV25 controls (Fig. 3*B*). The specificity of the antibody to Bak was shown by the absence of the ~30 kDa band in tissue extracts of *bak*$^{-/-}$ mouse brain (Fig. 6*B*). Baseline levels of Bax, detected at ~23 kDa, were similar in control DIV5 and DIV25 cortical neurons (Fig. 3*A*,*C*), but DIV5 and DIV25 neurons differed in their Bax responses induced by CPT. This ~23 kDa band is absent in *bax*$^{-/-}$ mouse brain extracts (Martin et al. 2003). Bax was increased ~6-fold and ~4-fold after 1 h of CPT exposure in DIV5 and DIV25 neurons, respectively (Fig. 3*A*,*C*). By 2 h exposure, the Bax increase was dissipating in DIV5 neurons, although still elevated above control level, whereas in DIV25 neurons the Bax increase above control was more sustained than in DIV5 neurons (Fig. 3*A*,*C*). DIV5 and DIV25 neurons had different baseline levels of Puma, detected at ~20 kDa (this immunoreactive band is absent in Western blots of liver extracts of *puma*$^{-/-}$ mice, data not shown); Puma was significantly higher in control DIV25 neurons compared with DIV5 neurons (Fig. 3*A*,*D*). DIV5 and DIV25 neurons had strikingly different Puma responses after CPT. Puma levels were unchanged in DIV5 neurons at 1 h after CPT, but then levels increased progressively to achieve about a 5-fold elevation above control by 4 h after CPT (Fig. 3A,D). DIV25 neurons displayed an abrupt ~2-fold increase in Puma at 1 hour after CPT, and then levels declined progressively (Fig. 3*A*,*D*). The patterns of Noxa expression, detected at ~11 kDa, differed from the Puma patterns at baseline and in the responses induced by CPT (Fig. 3*D*,*E*). Noxa in control DIV5 neurons was greater than in control DIV25 neurons (Fig. 3*A*,*E*). DIV5 neurons displayed an abrupt almost 3-fold increase in Noxa at 1 and 2 h after CPT and then levels declined sharply (Fig. 3*A*,*E*). In DIV25 neurons, Noxa levels increased slowly compared with DIV5 neurons after CPT exposure but achieved an almost 5-fold elevation by 4 h (Fig. 3*A*,*E*).

Bax and Bak are Downstream Mediators of DNA Damage-Induced Apoptosis in Immature and Differentiated Cortical Neurons

We used genetic and small-molecule pharmacological manipulations to identify if Bax and Bak mediate cortical neuron apoptosis and to determine if their roles differ in neurons at different stages of differentiation. However, a caveat of our cell system is the possibility of selection of neurons inherently more resistant to stress. We first evaluated the baseline survival of *bax*- and *bak*-null neurons compared with wild-type neurons, *ATM*$^{-/-}$ neurons, and *p53*$^{-/-}$ neurons. Survival of *bax*-, *bak*-, and *p53*-null cortical neurons was significantly greater at DIV5 and DIV25 than wild-type neurons plated at similar densities and grown under identical conditions (Fig. 3*F*). *ATM*-null neurons were similar to wild-type neurons (Fig. 3*F*). Deletion of the *bax* or *bak* gene protected strongly against apoptosis in DIV5 and DIV25 neurons challenged with CPT (Fig. 3*G*). Generally, the neuroprotection was greater in DIV25 null cells. The apoptotic response was reconstituted in *bak*-null cells using a cell-permeable Bak-BH3 fusion peptide (Fig. 3*G*) that binds selectively to Bcl-xL and antagonizes its function in non-neuronal cells (Holinger et al. 1999). The reconstitution of apoptosis was achieved to greater levels in DIV25 neurons compared with DIV5 neurons (Fig. 3*G*). For controls, neurons were exposed to a Bak peptide with a mutated BH3 sequence where leucine-78 is replaced by alanine (Holinger et al. 1999). These neurons had a level of apoptosis similar to vehicle control (Fig. 3*I*). To confirm the direct role of Bax in driving apoptosis in both immature and mature cortical neurons, wild-type neurons were treated with cell-permeable Bax-channel blocker (Bombrun et al. 2003; Hetz et al. 2005) or Bax-inhibiting peptide (Sawada et al. 2003) prior to CPT exposure. To show drug/peptide specificity, treatment experiments with Bax-channel blocker and Bax-inhibiting peptide were done on *bax*$^{-/-}$ neuron cultures. No additional neuroprotection was observed over that provided by the null mutations (data not shown). Both of these Bax antagonists protect HeLa cells from apoptosis (Bombrun et al. 2003; Sawada et al. 2003) and both provided major neuroprotection in

3 different culture experiments. Symbols denote: significantly lower $^{**}P < 0.001$ and $^{*}P < 0.01$ versus wild-type neurons. (*E*) Pharmacological inactivation of p53 reduces apoptosis in immature and mature wild-type cortical neurons. Neurons were treated (10 μM) with cyclic-α-pifithrin (α-PFT) that blocks reversibly p53-dependent transactivation of p53-dependent responsive genes, μ-PFT that blocks p53 interaction with Bcl-xL and Bcl-2 and inhibits selectively p53 translocation to mitochondria without affecting the transactivation function of p53, or a combination of both drugs for 2 h before exposure to 10 μM CPT. At 24 h, neurons were assessed for apoptosis. Values are mean ± SD based on at least 6 images of Hoechst-stained neurons per group and were replicated in 3 different culture experiments. Symbols denote: significantly lower $^{**}P < 0.001$ and $^{*}P < 0.05$ versus vehicle-treated neurons. (*F*) CPT-induced apoptosis of immature cortical neurons (but not mature cortical neurons) is transcriptionally and translationally dependent. Neurons were treated with the protein synthesis inhibitor cycloheximide (1 μg/ml) or the RNA synthesis inhibitor actinomycin D (1 μg/ml) for 2 h before exposure to 10 μM CPT. At 24 h, neurons were assessed for apoptosis. Values are mean ± SD based on at least 6 images of Hoechst-stained neurons per group and were replicated in 2 different culture experiments. Symbol denotes significantly lower $^{*}P < 0.001$ versus vehicle-treated neurons.

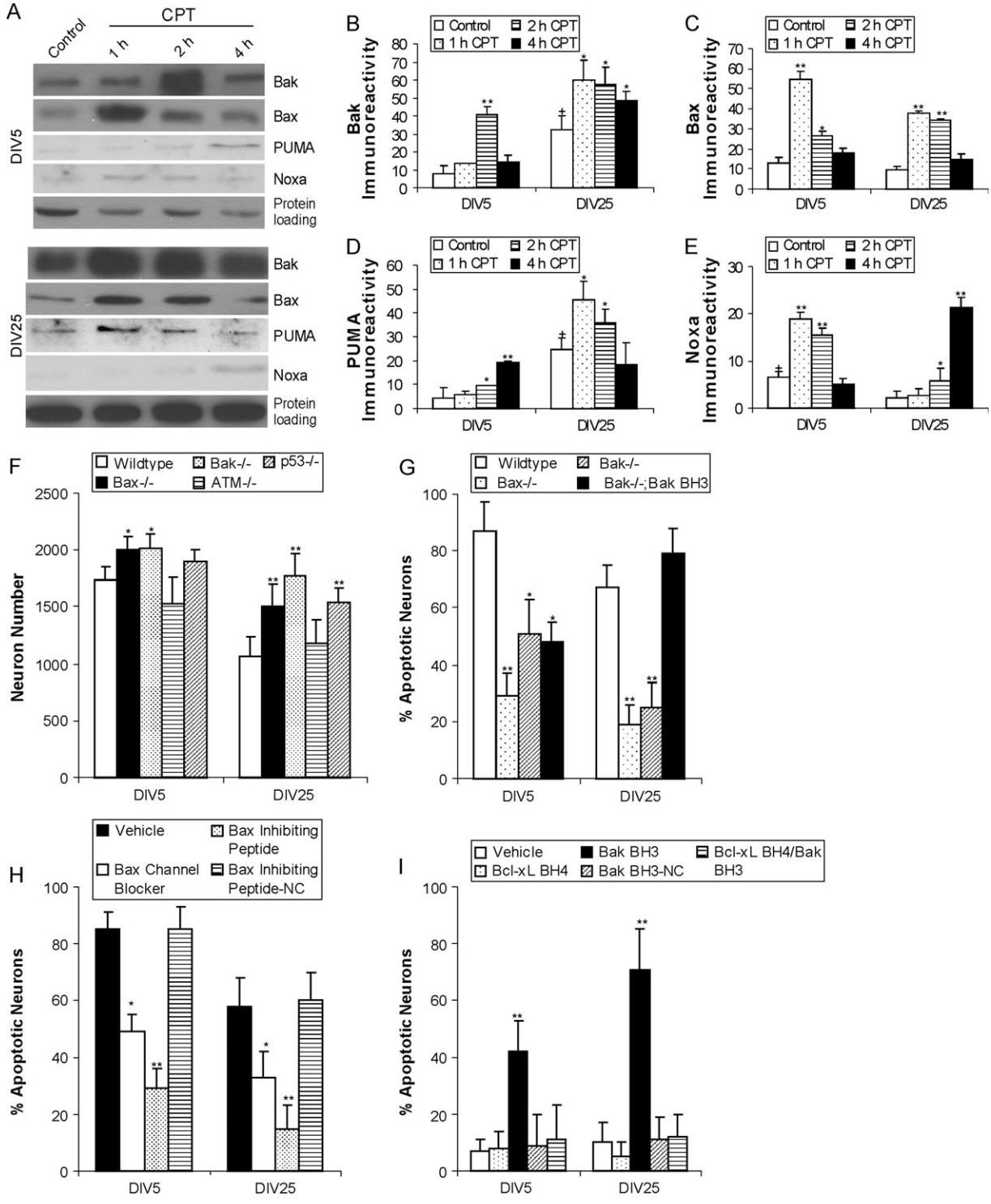

Figure 3. Effectors of cell death downstream of p53 are regulated differentially and have different contributions in the mechanisms of apoptosis in immature and mature cortical neurons. (*A*) Western blots showing rapid changes in the levels of multidomain (Bax and Bak) and BH3-only (Noxa and Puma) cell death proteins with 10 μM CPT treatment for 1 through 4 h in DIV5 and DIV25 neurons. GAPDH blot shows protein loading. (*B*) Graph of Bak levels (in relative OD units) in DIV5 and DIV25 neurons with 10 μM CPT treatments for 1 through 4 h. Values are mean ± SD ($n = 3$ different cultures of 6 pooled 35 mm wells per data point). Symbols denote: significantly higher $^{**}P < 0.001$ and $^{*}P < 0.01$ versus age-matched vehicle-treated neurons; significantly greater $^{+}P < 0.01$ versus DIV5 vehicle-treated neurons. (*C*) Graph of Bax levels (in relative OD units) in DIV5 and DIV25 neurons with 10 μM CPT treatments for 1 through 4 h. Values are mean ± SD ($n = 3$ different cultures of 6 pooled 35 mm wells per data point). Symbols denote: significantly higher $^{**}P < 0.001$ and $^{*}P < 0.01$ versus age-matched vehicle. (*D*) Graph of Puma levels (in relative OD units) in DIV5 and DIV25 neurons with 10 μM CPT treatments for 1 through 4 h. Values are mean ± SD ($n = 3$ different cultures of 6 pooled 35 mm wells per data point). Symbols denote: significantly higher $^{**}P < 0.01$ and $^{*}P < 0.05$ versus age-matched vehicle; significantly greater $^{+}P < 0.01$ versus DIV5 vehicle-treated neurons. (*E*) Graph of Noxa levels (in relative OD units) in DIV5 and DIV25 neurons with 10 μM CPT treatments for 1 through 4 h. Values are mean ± SD ($n = 3$ different cultures of 6 pooled 35 mm wells per data point). Symbols denote: significantly higher $^{**}P < 0.001$ and $^{*}P < 0.05$ versus age-matched vehicle; significantly greater $^{+}P < 0.05$ versus DIV25 vehicle-treated neurons. (*F*) Graph of the survival (neuron number/mm^2) of genetically distinct mouse cortical neurons with homozygous deletion of *Bax*, *Bak*, *ATM*, or *p53* genes compared with wild-type neurons. Neurons were plated at identical densities,

immature and mature *bax*$^{+/+}$ neurons (Fig. 3*H*). A mutated analog of the Bax-inhibiting peptide harboring no apoptotic activity (Sawada et al. 2003) had no effect on CPT-induced neuronal apoptosis (Fig. 3*H*).

It has been proposed that Bax and Bak can interact with the mitochondrial outer membrane protein VDAC to cause apoptosis (Shimizu et al. 2000). To examine the contribution of the VDAC in Bak-mediated neuronal apoptosis, wild-type DIV5 and DIV25 were treated with a cell-permeable peptide containing the conserved N-terminal Bcl-2 homology domain (BH4) of Bcl-xL (Bcl-xL-BH4) that prevents apoptosis by binding to the VDAC and blocking its activity in non-neural cells (Shimizu et al. 2000). Bcl-xL-BH4 peptide protected robustly against Bak-mediated apoptosis in cortical neurons (Fig. 3*I*).

DNA Damage Response Kinases Drive CPT-Induced p53-Mediated Apoptosis in Cortical Neurons

The mechanisms of cortical neuron apoptosis upstream of p53 activation were examined. Phosphorylation of p53 is a critical part of its activation sequence in response to DNA damage (Giaccia and Kastan 1998) and is mediated by about 5–10 different protein kinases, among them are ATM, ATR, and c-Abl (Kastan and Lim 2000). The ATM signaling network can be studied by tracking the phosphorylation of ATM and its substrates. To examine the overall phosphorylation status of proteins that are phosphorylated by ATM and the closely related kinase ATR, we did an ATM/ATR phosphorylated substrate screen of proteins from total cell lysates of wild-type cortical neurons treated with CPT for different times (Fig. 4*A*). In DIV5 neurons the phosphorylation of ATM/ATR substrate proteins, ranging from 17 kDa to 214 kDa, was increased significantly at 8 h (~150% of control) through 24 h (~250% of control) of CPT treatment (Fig. 4*A*). The pattern of ATM/ATR substrate protein phosphorylation was very different temporally and quantitatively in DIV25 neurons treated with CPT compared with DIV5 neurons treated similarly. In differentiated neurons, markedly increased (~300% of control) phosphorylation of ATM/ATR substrate proteins was seen at 4 h of CPT treatment, particularly a protein band at ~37 kDa (Fig. 4*A*). The phosphorylation of proteins in the range of 40 kDa to 200 kDa increased progressively from 4 h to 15 h in DIV25 neurons and then was dissipating at 24 h (Fig. 4*A*).

We next examined directly the activation of ATM in cortical neurons. DNA strand breaks can cause rapid activation of ATM through autophosphorylation at serine-1981 (Kastan and Lim 2000). Baseline activation of ATM, seen as a protein band at ~350–370 kDa, was very low in immature and differentiated control neurons (Fig. 4*B*). Antibody specificity was confirmed by the absence of this band of immunoreactivity in ATM$^{-/-}$ neurons (data not shown) and the robust immunoreactivity detected in irradiated HeLa cells (Fig. 4*B*). In DIV5 neurons challenged with CPT, phospho-ATM^{Ser1981} immunoreactivity was elevated transiently ~10-fold greater than control levels at 4 h but then was ~5-fold higher at 8 h, and subsequently levels dropped below control at 15 and 24 h (Fig. 4*B*). These increases in phospho-ATM occurred in the absence of significant elevations in the overall levels of ATM as detected with pan-ATM antibody. The temporal profile of ATM activation was different in DIV25 neurons. DIV25 neurons treated with CPT displayed phospho-ATM^{Ser1981} levels that were elevated robustly ~10-fold above control level from 4 h through 15 h and levels were still ~6-fold greater than control at 24 h (Fig. 4*B*).

The non-receptor tyrosine protein tyrosine kinase c-Abl can directly phosphorylate p53, and ATM can mediate p53 phosphorylation through ATM phosphorylation of c-Abl (Nakagawa et al. 1999). To investigate the possible role of c-Abl in the p53 activation sequence in CPT-treated cortical neurons, we examined the phosphorylation of c-Abl at tyrosine residue 245 which is involved in activation of c-Abl kinase activity (Kharbanda et al. 1998). Differentiating and mature cortical neurons at baseline have high levels of c-Abl as detected at ~135 kDa with phosphorylation state-specific and phosphorylation-independent antibodies, but active c-Abl is higher in immature neurons (Fig. 4*C*). DIV5 neurons treated with CPT had sharply decreased (~62% of control) levels of phospho-c-Abl^{Tyr245} at 4 h and then subsequently a partial recovery of phospho-c-Abl^{Tyr245} levels by 8 h and thereafter but with levels still reduced significantly to ~80% of control (Fig. 4*C*). In contrast, DIV25 neurons treated with CPT had levels of phospho-c-Abl^{Tyr245} ~1.5-fold higher than control at 4, 8, and 15 h but then levels declined markedly to 36% of control by 24 h (Fig. 4*C*).

We next examined the relationship between ATM and specific substrate protein phosphorylation. p53 was immunoprecipitated from CPT-treated DIV5 and DIV25 cortical neuron lysates with a pan-p53 antibody, and then immunoprecipitated protein was Western blotted using ATM/ATR phosphosubstrate antibody. ATM/ATR phosphorylated-p53 was elevated above control levels at 4, 8, and 15 h in DIV5 neurons and at 4 and 8 h in DIV25 neurons (Fig. 4*D*). We were not able to immunoprecipitate c-Abl from CPT-treated DIV5 cortical neurons, mostly likely because of its reduced levels. However c-Abl in CPT-treated DIV25 neurons was an ATM/ATR phosphosubstrate and its phosphorylation was increased markedly with CPT treatment (Fig. 4*D*).

Cortical neuron apoptosis was studied in the presence of genetic and pharmacological inactivation of ATM or c-Abl.

maintained identically in culture, and then assessed for survival at DIV5 and DIV25 using phase contrast imaging. Values are mean ± SD based on at least 6 images per group and were replicated in 2 different culture experiments. Symbols denote: significantly higher $*P < 0.05$ and $**P < 0.01$ versus age-matched wild-type neurons. (*G*) Homozygous deletion of *Bax* or *Bak* genes protect against apoptosis in mouse cortical neurons treated with CPT for 24 h at DIV5 and DIV25. Apoptosis was reconstituted in *Bak*$^{-/-}$ mouse cortical neurons by treatment (20 μM) with a cell-permeable Bak-BH3 domain peptide. Mutated Bak-BH3 peptide (negative control, NC) had no apoptotic activity in cortical neurons (see panel I). Values are mean ± SD based on at least 6 images of Hoechst-stained neurons per group and were replicated in 3 different culture experiments. Symbols denote: significantly lower $**P < 0.001$ and $*P < 0.01$ versus wild-type neurons. (*H*) Neuroprotection in wild-type mouse cortical neurons by pharmacological manipulation of Bax function. Pretreatment (20 μM) of DIV5 and DIV25 cortical neurons with a cell-permeable Bax-channel blocker (dibromocarbazole-piperazinyl derivative) or a Bax-inhibiting pentapeptide derived from the Ku70-Bax inhibiting domain effectively blocks CPT-induced apoptosis. A mutated analog of Bax-inhibiting pentapeptide did not block apoptosis of cortical neurons. Values are mean ± SD based on at least 6 images of Hoechst-stained neurons per group and were replicated in 3 different culture experiments. Symbols denote: significantly lower $**P < 0.001$ and $*P < 0.01$ versus vehicle-treated neurons exposed to 10 μM CPT. (*I*) Neuroprotection in wild-type mouse cortical neurons using an antiapoptotic BH4 domain peptide. Pretreatment (10 μM) with a peptide containing the Bcl-X_L-BH4 domain linked to a 10 amino acid HIV-TAT carrier peptide (Bcl-X_L-BH4 peptide) completely blocked Bak-BH3 peptide-induced (20 μM) apoptosis. Values are mean ± SD based on at least 6 images of Hoechst-stained neurons per group and were replicated in 3 different culture experiments. Symbols denote: significantly higher $**P < 0.001$ than all other treatment groups.

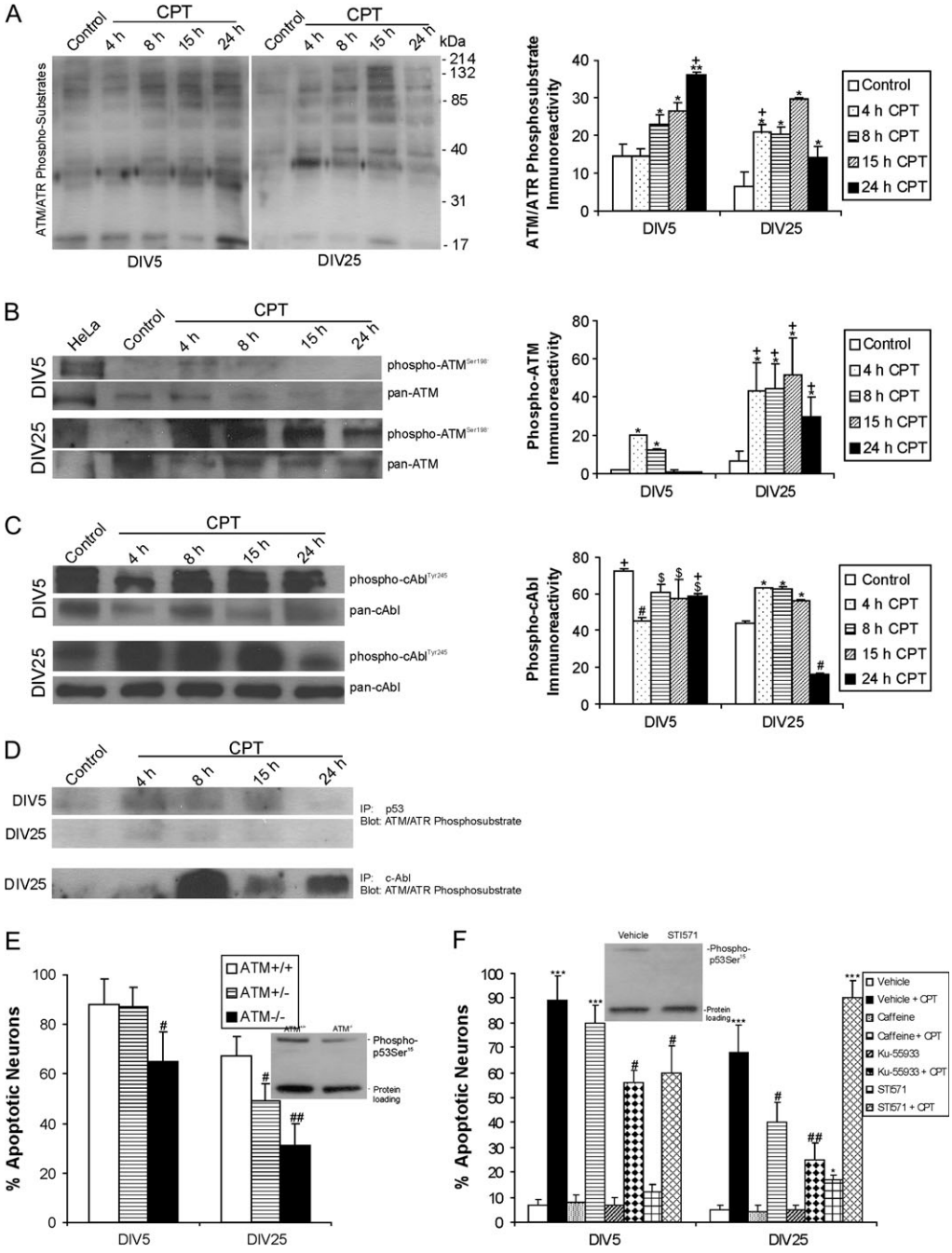

Figure 4. DNA damage response kinases drive CPT-induced p53-mediated apoptosis in immature and mature cortical neurons. A. Western blots show activation of ATM/ATR kinase (by detection of phosphorylated substrate proteins) after CPT treatment (10 μM) for 4 through 24 h (h) in DIV5 and DIV25 neurons. Graph of ATM/ATR phosphosubstrate immunoreactivity (in relative OD units) in DIV5 (immature) and DIV25 (mature-differentiated) neurons with 10 μM CPT treatment. Values are mean ± SD ($n = 3$ different cultures of 6 pooled 35 mm wells per data point). Symbols denote: significantly greater $^{**}P < 0.001$ and $^{**}P < 0.01$ versus age-matched vehicle; significantly greater $^{+}P < 0.01$ versus time-matched CPT-treated neurons. (*B*) Western blots show robust activation of ATM through phosphorylation of serine-1981 (detected with phosphorylation state-specific antibody) after 10 μM CPT treatment for 4 through 24 h in DIV5 and DIV25 neurons. Total levels of ATM (detected with a phosphorylation state-independent pan antibody) decrease over time. γ-Irradiated HeLa cells are a positive control for DNA damaged-induced activation of ATM. Graph of phospho-ATM levels (in relative OD units) in DIV5 (immature) and DIV25 (mature-differentiated) neurons with 10 μM CPT treatment. Values are mean ± SD ($n = 3$ different cultures of 6 pooled 35 mm wells per data point). Symbols denote: significantly greater $^{*}P < 0.01$ versus age-matched vehicle; significantly greater $^{+}P < 0.05$ than time-matched DIV5 neurons. (*C*) Western blots for activated tyrosine-245-phosphorylated c-Abl (detected with phosphorylation state-specific antibody) and total c-Abl (detected with a phosphorylation state-independent pan antibody) with 10 μM CPT treatment for 4 through 24 h (h) in DIV5 and DIV25 neurons. Graph of phospho-cAbl levels (in relative OD units) in DIV5 (immature) and DIV25 (mature-differentiated) neurons with 10 μM CPT treatment. Values are mean ± SD ($n = 3$ different cultures of 6 pooled 35 mm wells per data point). Symbols denote: significantly lower $^{\#}P < 0.001$ and $^{\$}P < 0.05$ versus age-matched vehicle-treated neurons; significantly greater $^{*}P < 0.01$ versus age-matched vehicle-treated neurons; significantly greater $^{+}P < 0.01$ than time-matched DIV25 neurons. (*D*) Immunoprecipitation assay identifying p53 and c-Abl as direct ATM/ATR targets in cortical neurons undergoing apoptosis induced by CPT. Results were confirmed in 3 different experiments. (*E*) *ATM* gene deletion provides significant protection against apoptosis in DIV5 and DIV25 cortical neurons treated with CPT for 24 h. Values are mean ± SD based on at least 6 images of Hoechst-stained neurons per group and were replicated in 3 different culture experiments. Symbols denote: significantly lower $^{\#}P < 0.05$ and $^{\#\#}P < 0.01$ versus wild-type neurons. Western blot shows that *ATM* gene deletion attenuates p53 activation. (*F*) Pharmacological inactivation of ATM and c-Abl protects against apoptosis in immature and mature wild-type cortical neurons. Neurons were treated with highly specific (Ku-55933, 10 μM) or less specific

Neuron cultures were prepared from wild-type, $ATM^{+/-}$, and $ATM^{-/-}$ mouse embryos, maintained for 5 or 25 days, and treated with 10 μM CPT for 24 h. The apoptotic response of $ATM^{-/-}$ DIV5 cortical neurons was attenuated modestly (~23% protection), whereas that of $ATM^{+/-}$ neurons at DIV5 was not affected (Fig. 4*E*). In contrast, DIV25 neurons with no ATM were protected robustly from apoptosis (~40%) and hemizygous neurons showed slight protection (Fig. 4*E*). The activation of p53 in response to CPT was attenuated in $ATM^{-/-}$ DIV25 neurons (Fig. 4*E*). Wild-type cortical neurons were then treated prior to CPT exposure with Ku-55933 or caffeine which are highly specific (Hickson et al. 2004) or less specific (Blasina et al. 1999) inhibitors of ATM kinase activity, respectively. Neither drug had significant effect on the amount of apoptosis in CPT-treated DIV5 neurons (Fig. 4*F*). In contrast, both Ku-55933 and caffeine afforded significant protection to CPT-treated DIV25 neurons (Fig. 4*F*). As control experiments for ATM drug specificity, treatment experiments with Ku-55933 and caffeine were repeated in $ATM^{-/-}$ neuron cultures but no additional actions were observed (data not shown).

c-Abl null neurons were unavailable for our experiments, but we used a highly selective inhibitor of c-Abl (Raina et al. 2002) to examine the involvement of c-Abl in cortical neuron apoptosis. CPT-induced apoptosis in DIV5 neurons was attenuated modestly when c-Abl was inhibited with STI571, but apoptosis was worsened in DIV25 neurons in the presence of c-Abl inhibition (Fig. 4*F*). The activation of p53 in response to CPT was prominently blocked in DIV5 neurons treated with STI571 (Fig. 4*F*).

Immature Neurons are More Sensitive than Differentiated Neurons to DNA Damage

To better identify possible differences in the vulnerabilities of immature neurons and differentiated neurons to DNA-damaging insults, DIV5 and DIV25 cortical neurons were treated with a submicromolar concentration of CPT for longer than 24 h (Fig. 5*A*). CPT at a concentration of 0.5 μM induced a time-dependent accumulation of apoptotic DIV5 and DIV25 cortical neurons. DIV25 neurons were about 50% less vulnerable than DIV5 neurons to the toxicity of CPT over 72 h (Fig. 5*A*). We used ETOP as a different toxin to determine if the greater vulnerability of immature neurons compared with more mature neurons is a general rule. ETOP at a concentration of 0.5 μM also induced a time-dependent accumulation of apoptotic DIV5 and DIV25 cortical neurons, and, once again, differentiated neurons were significantly less vulnerable than immature neurons (Fig. 5*B*). This low-dose, time-based experiment reveals that immature neurons are significantly more sensitive than differentiated neurons to DNA-damaging agents (Fig. 5*A*,*B*).

Apoptosis in Cultured Cortical Neurons Triggered by ETOP is also Driven by p53, ATM Kinase, and Bcl-2 Family Members

To affirm that the molecular mechanisms driving apoptosis in cortical neurons are related to DNA damage rather than being CPT-specific, we repeated some key experiments using ETOP to induced DNA damage and apoptosis in DIV5 and DIV25 cortical neurons.

DIV5 and DIV25 cortical neurons were treated with 1, 10, or 100 μM ETOP or with vehicle and then evaluated for apoptosis after 24 h (Fig. 5*C*). ETOP-induced apoptosis in cortical neurons at all concentrations (Fig. 5*C*) that was similar morphologically (data not shown) to CPT-induced apoptosis (Fig. 1*A*). The amount of ETOP-induced apoptosis in cortical neuron cultures was dose-dependent (Fig. 5*C*). DIV25 neurons were less sensitive than DIV5 neurons at the 10 and 100 μM doses (Fig. 5*C*).

ETOP-treated neurons were evaluated for the presence of DNA-DSBs using the neutral comet assay (Martin and Liu 2002). In both DIV5 and DIV25 cortical neurons DNA-DSBs accumulated significantly with 4 h of ETOP exposure (Fig. 5*D*). Comet counts revealed that immature neurons accumulate more DNA-DSBs compared with differentiated neurons after 10 μM ETOP exposure (Fig. 5*D*).

The mechanisms of ETOP-induced apoptosis of cortical neurons involving p53 and its downstream and upstream signaling pathways were analyzed, as done for CPT. Cortical neuron cultures were prepared from wild-type and $p53^{-/-}$ mouse embryos, maintained for 5 or 25 days, and treated with 10 μM ETOP for 24 h. Apoptosis of $p53^{-/-}$ DIV5 neurons was blocked nearly 90%, whereas the apoptotic response of $p53^{-/-}$ DIV25 neurons was blocked by about 40% (Fig. 5*E*). DIV5 and DIV25 neurons without *bax* or *bak* genes also showed attenuated apoptosis after exposure to ETOP (Fig. 5*F*). The apoptotic response in *bak*-null cells was also reconstituted using Bak–BH3 fusion peptide (Fig. 5*F*). Apoptosis of DIV5 and DIV25 cortical neurons without $ATM^{-/-}$ was attenuated significantly after ETOP exposure, whereas $ATM^{+/-}$ neurons were unaffected (Fig. 5*G*). Cortical neurons were then treated prior to ETOP exposure with ATM kinase inhibitors (Ku-55933 or caffeine). Both drugs had significant effects on the amount of apoptosis in ETOP-treated DIV5 neurons and DIV25 neurons (Fig. 5*H*). ETOP-induced apoptosis in DIV5 neurons was attenuated significantly by the c-Abl inhibitor STI571, but the amount of apoptosis was unaffected in DIV25 neurons in the presence of c-Abl inhibition (Fig. 5*H*).

Cell Death Proteins are Regulated Differentially in Developing Mouse Forebrain

Another caveat of our cell system is whether neuron maturation in culture is similar to neuron maturation in vivo. To begin to establish the relevancy of our findings on cultured cortical neurons to the intact brain setting, we analyzed the expression of selected cell death proteins in mouse forebrain during normal maturation and in response to CPT (Fig. 6). For phospho-p53, Bax, Bak, and Noxa, the general pattern was highest levels at P0 followed by progressive declines in levels as the forebrain matured postnatally (Fig. 6*A*), but they were still detectable in P20 forebrain. In contrast, Puma protein levels increased progressively in forebrain as maturation proceeded (Fig. 6*A*).

(caffeine, 100 μM) ATM inhibitors or the c-Abl inhibitor (STI571, 10 μM) for 2 h before exposure to 10 μM CPT. At 24 h, the neurons were assessed for apoptosis. Values are mean ± SD derived from at least 6 images of Hoechst-stained neurons per group and were replicated in 3 different culture experiments. Symbols denote: significantly higher $^{***}P < 0.001$ and $^{*}P < 0.05$ versus age-matched vehicle-treated neurons; significantly lower $^{\#}P < 0.01$ and $^{\#\#}P < 0.001$ versus age-matched CPT/vehicle-treated neurons. Western blotting shows that p53 activation is attenuated by c-Abl inhibition. ATM inhibition also attenuated p53 activation (data not shown).

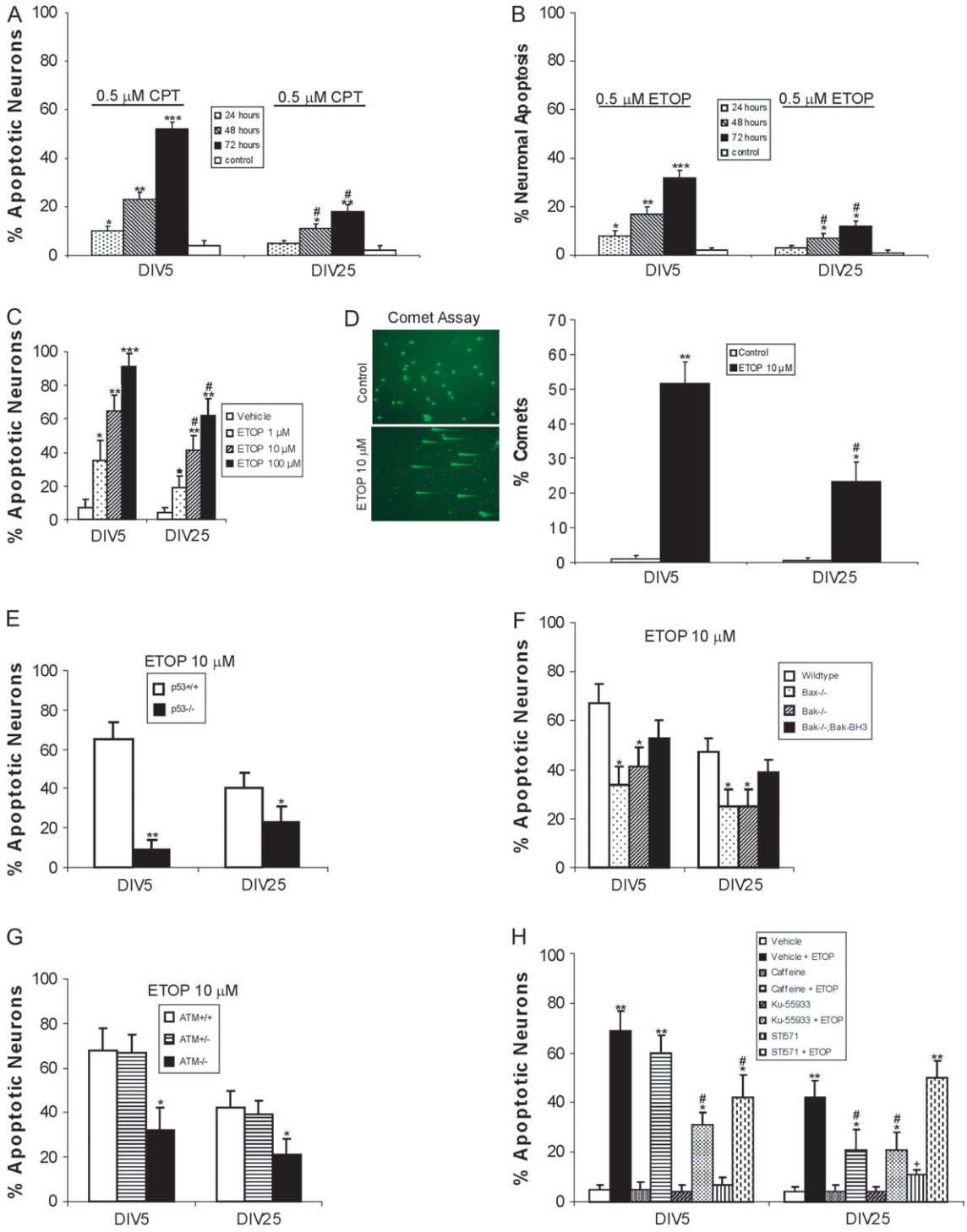

Figure 5. Low-dose CPT and an alternative DNA-damaging agent, ETOP, induce apoptosis of cortical neurons and reveal that undifferentiated neurons have greater sensitivity than differentiated neurons to DNA damage. (*A*, *B*) Mouse cortical neuron apoptosis is time and maturity dependent with exposure to low-dose CPT (*A*) or ETOP (*B*). Graphs show the amount of apoptosis in DIV5 (immature) and DIV25 (mature-differentiated) neurons after exposure to 0.5 μM CPT or 0.5 μM ETOP for 24, 48, or 72 h. Values are mean ± SD based on at least 6 images per group. Results were replicated in 3 different cell culture experiments. Symbols denote: significantly greater $^{*}P < 0.05$, $^{**}P < 0.005$, and $^{***}P < 0.001$ versus control; significantly lower $^{\#}P < 0.05$ versus time-matched DIV5 neurons. (*C*) The amount of cortical neuron apoptosis induced by ETOP is dose-dependent in DIV5 (immature) and DIV25 (mature-differentiated) neurons. Graph shows the percentage of apoptotic neurons (mean ± SD) determined from 6 images per group. Results were replicated in 3 different cell culture experiments. Symbols denote: significantly greater $^{*}P < 0.05$, $^{**}P < 0.005$, and $^{***}P < 0.005$ versus vehicle; significantly lower $^{\#}P < 0.05$ versus concentration-matched DIV5 neurons. (*D*) Neutral comet assay showing the accumulation of DNA-DSBs in immature DIV5 neurons after 4 h exposure to 10 μM ETOP. DNA is stained with SYBR-Green. No control neurons have comet tails. Many ETOP-treated neurons have comet tails indicating DNA-DSBs. Graph shows the percentage of DIV5 and DIV25 neurons with DNA-DSBs after 4 h exposure to 10 μM ETOP as determine by neutral comet assay. Values are mean ± SD, based on at least 10 images per group and were replicated in 2 different culture experiments and comet assays. Symbols denote: significantly greater $^{*}P < 0.005$, $^{**}P < 0.001$; significantly lower $^{\#}P < 0.01$ versus DIV5 neurons. (*E*) *p53* gene deletion reduces significantly the amount of apoptosis in DIV5 and DIV25 cortical neurons treated with ETOP for 24 h. Values are mean ± SD based on at least 6 images of Hoechst-stained neurons per group and were replicated in 2 different culture experiments. Symbols denote: significantly lower $^{**}P < 0.001$ and $^{*}P < 0.05$ versus wild-type neurons. (*F*) Mouse cortical neurons without *Bax* or *Bak* genes are protected from apoptosis when treated with ETOP for 24 h at DIV5 and DIV25. Apoptosis is

DNA Damage Induces p53 Activation, Elevated Mitochondrial Cell Death Proteins, and Widespread Apoptosis in Cerebral Cortex of Mice

An additional caveat of our neuronal cell system is whether the molecular regulation of apoptosis in cultured neurons is representative of events occurring in brain. In P5 mice treated with CPT, p53 phosphorylation in cerebral cortex was elevated compared with control by 8 h after intraventricular CPT infusion and was increased further by 16 h (Fig. 6*B*). Bax and Bak were also increased in cerebral cortex after in vivo CPT treatment compared with vehicle treatment (Fig. 6*B*). The brains of mice treated with intraventricular CPT at P5 and killed 24 h later were atrophic, as revealed by dilation of the lateral ventricles and shrinkage of the forebrain, and had widespread apoptosis within the cerebral cortex (Fig. 6*C*). Importantly, the morphology of the cellular degeneration in cerebral cortex induced by CPT was entirely apoptotic, similar to that occurring in cultured cortical neurons treated with CPT. There was no evidence for necrotic cell death or, surprisingly, apoptosis-necrosis hybrid cell deaths that occur in other rodent models of cortical neuron degeneration induced by excitotoxicity or hypoxia-ischemia (Portera-Cailliau et al. 1997; Northington et al. 2007).

Discussion

It is not known whether DNA damage initiates cell death in postmitotic cortical neurons and how this occurs. Our study is important because it implicates strongly the accumulation of DNA strand breaks as a major triggering event for neuronal apoptosis. We then delineated the molecular mechanisms of DNA damage-induced apoptosis upstream and downstream of p53 in cortical neurons at immature and differentiated states.

DNA Strand Break Accumulation is a Candidate Initiator of Apoptosis in Undifferentiated and Differentiated Cortical Neurons

Cortical neurons accumulate high levels of DNA strand breaks within 4 h exposure to Topo inhibitors. It is likely that the strand breaks accumulate before 4 h because p53 phosphorylation is enhanced by 1 h. This outcome is not drug-specific and the apoptosis is most likely induced by the DNA strand breaks. These events occur in both immature DIV5 neurons and well-differentiated DIV25 neurons in a dose-dependent fashion. Immature neurons are more prone than mature neurons to accumulate DNA-SSBs. Maturity-related differences in vulnerability to DNA strand break accumulation could be due to acquisition of proficient DNA repair mechanisms in more mature neurons (Romero et al. 2003) or to differences in constitutive levels of topoisomerase isoforms in cortical neurons. Topo-I protein is depleted rapidly in cortical neurons exposed to CPT, similar to cycling cells (Nieves-Neira et al. 1999); thus, interference with RNA transcription could be involved also in cortical neuron apoptosis. The high vulnerability for postmitotic neurons to accumulate DNA-SSBs, apparently dissociated from S-phase DNA replication, could be related to their high level of RNA synthesis, and thus a greater dependence on Topo-I. The rapid accumulation of DNA strand breaks in this neuronal model places DNA damage as an activator of an ATM/p53-regulated apoptosis cascade.

DNA Damage Sensor Kinase ATM Regulates Apoptosis in Cortical Neurons

Our conclusion that DNA damage is an initiator of apoptosis in cortical neurons is supported strongly by data showing that the ATM/c-Abl-p53 signaling network is activated. Scant work has been done on the upstream signal transduction mechanisms in neurons that link DNA damage to p53 and apoptosis. ATM and ATR are DNA damage sensor kinases that become activated in response to DNA damage; p53 and c-Abl are among the identified substrates (Kastan and Lim 2000). In non-neuronal human cells, ATM is activated by phosphorylation and is required for the phosphorylation of p53 at serine^{15} and serine^{20} (Dumaz et al. 2001). Neonatal mice without ATM have reduced p53-mediated brain neuron apoptosis in response to DNA damage from ionizing radiation (Lee et al. 2001), but responses of *ATM*-null brain neurons to other genotoxins are not known. We show that ATM is activated, and ATM/ATR protein substrates are phosphorylated during apoptosis in cortical neurons. Importantly, *ATM*-null neurons are protected from apoptosis, demonstrating a direct role for ATM in cortical neuron apoptosis. Moreover, inhibitors of ATM kinase activity are antiapoptotic in cortical neurons (Fig. 7). One earlier study has shown that *ATM*-null DIV14 cortical neurons are resistant to apoptosis induced by excitotoxicity (Macleod et al. 2003). Another study has shown that ATM phosphorylates p53 and drives apoptosis in DIV2 cortical neurons exposed to CPT (Keramaris et al. 2003). We know now that the activation of ATM and the requirement of ATM for DNA damaged-induced apoptosis are greater in differentiated neurons compared with immature neurons (Fig. 7).

c-Abl—A Novel Regulator of Cortical Neuron Apoptosis

DNA damage is also linked to p53 and apoptosis through the non-receptor tyrosine kinase c-Abl. c-Abl is activated by DNA damage and binds p53 causing increased transactivation function (Kharbanda et al. 1998). Phosphorylation of c-Abl by ATM and DNA-PK activates its kinase activity. Deletion of c-Abl and inhibition of c-Abl with STI571 can block apoptosis of non-neural cells (Raina et al. 2002). We show that c-Abl is activated

reconstituted in *Bak*$^{-/-}$ mouse cortical neurons by treatment (20 μM) with a cell-permeable Bak-BH3 domain peptide. Mutated Bak-BH3 peptide had no apoptotic activity in cortical neurons (data not shown). Values are mean ± SD based on at least 6 images of Hoechst-stained neurons per group and were replicated in 3 different culture experiments. Symbols denote: significantly lower $^{*}P < 0.01$ versus wild-type neurons. (*G*) Mouse cortical neurons without the *ATM* gene have significantly less apoptosis at DIV5 and DIV25 when treated with ETOP for 24 h. Values are mean ± SD based on at least 6 images of Hoechst-stained neurons per group and were replicated in 3 different culture experiments. Asterisk denotes significantly lower $P < 0.01$ (DIV5) or $P < 0.05$ (DIV25) versus *ATM*$^{+/+}$ neurons. (*H*) Small-molecule inhibitors of ATM or c-Abl kinases alter ETOP-induced apoptosis outcome in immature and mature wild-type cortical neurons. Neurons were treated with ATM inhibitors Ku-55933 (10 μM) or caffeine (100 μM) or the c-Abl inhibitor (STI571, 10 μM) for 2 h before exposure to 10 μM ETOP. At 24 h, the neurons were assessed for apoptosis. Values are mean ± SD derived from at least 6 images of Hoechst-stained neurons per group and were replicated in 3 different culture experiments. Symbols denote in DIV5 groups significantly higher $^{**}P < 0.001$ and $^{*}P < 0.01$ versus age-matched vehicle-treated neurons and significantly lower $^{\#}P < 0.01$ versus ETOP/vehicle-treated neurons. Symbols denote in DIV25 groups significantly higher $^{**}P < 0.01$ and $^{*}P < 0.05$ versus age-matched vehicle-treated neurons, significantly lower $^{\#}P < 0.05$ versus ETOP/vehicle-treated neurons, and significantly higher $^{+}P < 0.05$ than vehicle only treated control.

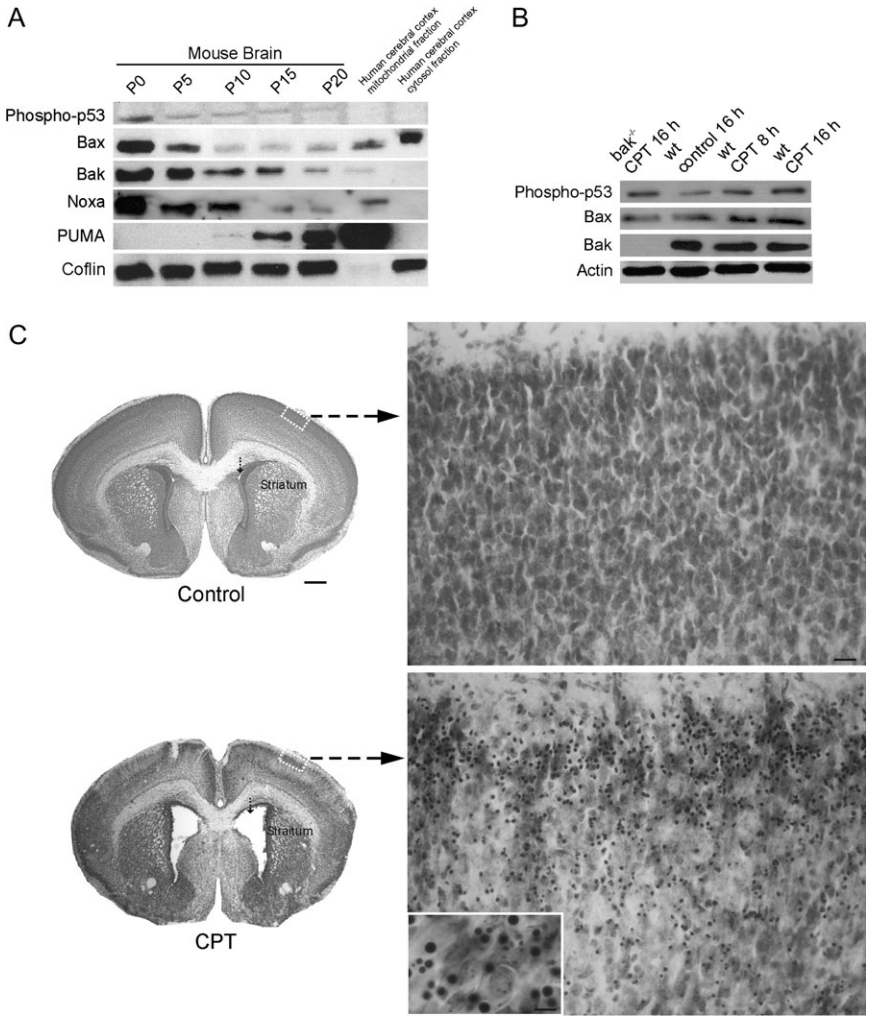

Figure 6. Cell death protein levels and activation in mouse brain during normal maturation and CPT-induced apoptosis. (*A*) Western blots of phospho^{Ser15}-p53, Bax, Bak, Noxa, and Puma in normal wild-type mouse forebrains on the day of birth (P0) and at postnatal (P) days 5, 10, 15, 20. Nuclear fractions (10 μg protein) were used for p53. Mitochondrial-enriched fractions (10 μg protein) were used for Bax, Bak, Noxa, and Puma. Blots were re-probed for cofilin to show equivalent protein loading (a representative blot for cofilin is shown). Mitochondrial and cytosolic fractions of adult human motor cortex are positive or negative controls for antibody specificity. (*B*) Western blots of phospho^{Ser15}-p53, Bax, and Bak in cerebral cortex of wild-type (wt) and *bak*-null mice injected intraventricularly with 10 μM CPT and killed at 8 or 16 h later. Blots were re-probed for actin to show equivalent protein loading (a representative blot for actin is shown). (*C*) Intraventricular CPT induces robust apoptosis in mouse brain. Wild-type P5 mice were injected in the right lateral ventricle (arrow) with 10 μM CPT ($n = 6$) or an equal volume of vehicle (control, $n = 6$) and were killed 24 h later. CPT-induced marked dilation of the lateral ventricles and shrinkage of the striatum. Numerous apoptotic cells were seen in cerebral cortex of CPT-treated mice (lower right panel and inset) but not in vehicle-injected mice (upper right panel). Scale bars: 500 μm (left panels); 22.5 μm (right panels); 5 μm (inset).

strongly in mature neurons with DNA damage. However, c-Abl inhibition with STI571 is neuroprotective in immature neurons but worsens the degeneration in mature neurons. We conclude that c-Abl is a regulator of apoptosis and survival in cortical neurons and that this role depends on neuronal differentiation state (Fig. 7).

The Actions of p53 in Driving Apoptosis in Cortical Neurons and the Dependence on Transcription-Translation is Influenced by Neuron Differentiation

We show that p53 is a major regulator of cortical neuron apoptosis. CPT exposure induces substantial phosphorylation and nuclear localization of p53 in cultured neurons, consistent with the presence of DNA damage. p53 activation is more robust in immature neurons compared with mature neurons, in keeping with the greater accumulation of DNA-SSBs in immature neurons. The apoptosis induced by CPT and ETOP is blocked in neurons without *p53* genes. The neuroprotection is greater in immature neurons compared with differentiated neurons. Inhibition of the DNA binding *trans*-activation function of p53 with α-PFT (Komarov et al. 1999) partially blocks apoptosis in immature and mature neurons (Fig. 7). Interestingly, blocking p53 interaction with Bcl-xL and Bcl-2 and inhibiting p53 translocation to mitochondria, without affecting the *trans*-activation function of p53 with μ-PFT (Strom et al. 2006), has very robust antiapoptotic effects in differentiated neurons (Fig. 7). Additional evidence that the nuclear trans-activation function of p53 is more important in immature neurons compared with differentiated neurons is the observation that inhibitors of RNA transcription and translation block apoptosis in immature neurons but not in differentiated neurons (Fig. 7). These data reveal the possibility that p53-mediated apoptosis in immature neurons is transcription-dependent, whereas p53-mediated apoptosis in differentiated

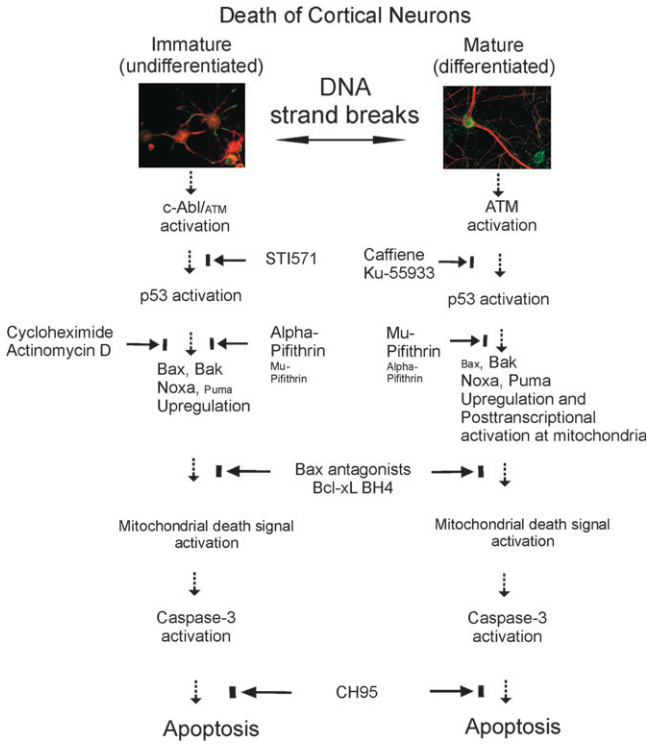

Figure 7. Summary diagram illustrating the molecular regulation of apoptosis in immature and differentiated cortical neurons induced by DNA damage. Differences in font sizes reflect the weight of the particular protein or inhibitor (the smaller the font the less involvement or magnitude of change).

neurons is transcription-independent (Fig. 7). p53 can mediate mitochondrial permeabilization through direct physical interaction with Bax and Bak (Chipuk et al. 2004). We conclude that p53 regulates DNA damage-induced apoptosis in both immature and mature cortical neurons, but p53 functions differently depending on neuron differentiation by having primarily a nuclear role in immature neurons and probably nuclear and mitochondrial roles in mature neurons (Fig. 7).

Earlier studies have shown that the tumor suppressor p53 can mediate neuronal death in cell culture. Overexpression of p53 causes neurodegeneration in cultures of sympathetic ganglion neurons (Slack et al. 1996), immature cerebellar granule neurons (Cregan et al. 1999), and cortical neurons (Xiang et al. 1996, 1998). CPT-induced death of DIV2–4 cortical neurons is blocked in cells deficient in p53 (Xiang et al. 1998). Another study has shown increased levels of p53 protein and increased p53 phosphorylation in DIV2 cortical neurons exposed to CPT (Keramaris et al. 2003). The involvement of p53 in neuronal apoptosis might be differential depending on cell type and cell maturity because the dependence of apoptosis on p53 in neurons might decline with maturation (Johnson et al. 1999), but this interpretation is confounded because the neuronal cultures were generated from different sources (embryonic and postnatal brains) with inherently different amenabilities to culture. A novel contribution of our work is the finding that immature neurons and differentiated mature neurons have some common molecular mechanisms for apoptosis with respect to p53 dependence, but they also exhibit key differences. Immature and mature cortical neurons do not undergo p53 activation equivalently, p53-mediated apoptosis in immature cortical neurons has greater transcriptional-translational dependence than in differentiated neurons, and p53 may function at mitochondria (thus bypassing transcriptional-translational dependence) in differentiated cortical neurons (Fig. 7).

Cortical Neuron Apoptosis is Dependent on Bax and Bak

Our study reveals several new aspects about the regulation apoptosis in cortical neurons by Bcl-2 family members. We demonstrate that Bax protein levels are increased several fold, surprisingly within one hour, in cultured cortical neurons treated with CPT; furthermore, both immature and differentiated neurons without Bax are protected strongly against DNA damage-induced apoptosis in vitro. Moreover, interruption of the Bax function with a Bax-channel blocker and a Bax-inhibiting peptide protects robustly wild-type immature and mature neurons, showing for the first time the antiapoptotic effects of small-molecules targeting Bax in cortical neurons at different stages of maturation (Fig. 7). We also show that Bax is upregulated in cerebral cortex after intracerebral exposure to CPT. The increase in the level of Bax protein is rapid and transient, thus it can be missed by studying an inappropriate time scale, and suggests that transcriptional mechanisms are engaged rapidly and/or there is an existing pool of Bax transcripts available for rapid translation. Previous reports have shown that CPT-induced death of cultured immature neurons involves proteins in the Bcl-2 family. Death of DIV1–2 or DIV4 cortical neurons induced by CPT is blocked in cells deficient in Bax (Xiang et al. 1998), and Bax-deficient cerebellar granule neurons in vitro are resistant to apoptosis induced by adenoviral overexpression of p53, indicating that Bax events are downstream of p53 (Cregan et al. 1999). The human *bax* gene promoter is activated directly by p53 (Miyashita and Reed, 1995), but there is some controversy about the role of p53 in direct transcriptional activation of the murine *bax* gene promoter and whether there are other p53-responsive binding sites in intronic sequences of the murine bax gene (Igata et al. 1999; Schmidt et al. 1999, Thornborrow et al. 2002). We find after CPT exposure an increase in Bax in cultured mouse neurons and in the mouse brain coinciding with the onset of p53 activation, suggesting that a commitment to apoptosis occurs very rapidly in cortical neurons in a p53-dependent manner, but we have not shown that p53 is directly causing the elevation in Bax.

We show for the first time that Bak, a close homologue of Bax, has a role in mediating apoptosis in cortical neurons. Bak protein is upregulated in cortical neurons undergoing apoptosis. Bak protein is also upregulated in mouse cerebral cortex during apoptosis in vivo. The transcriptional activity of p53 can enhance Bak expression (Pohl et al. 1999; Kannan et al. 2001). The operations of Bax and Bak in apoptotic immature and differentiated neurons appear to be different temporally based on their protein expression profiles. Neurons without Bak are protected against apoptosis; differentiated *bak*-null neurons show greater resistance than immature neurons. In addition, exposure of wild-type and *bak*-null cortical neurons to Bak–BH3 peptide induces apoptosis. Bak–BH3 mediated apoptosis is blocked fully by a fusion peptide that inhibits the VDAC (Shimizu et al. 2000), supporting an idea that Bak interacts with the mitochondrial permeability transition pore to induce its

opening and apoptosis in cortical neurons. Such an interaction has been seen in rat liver and yeast mitochondria (Shimizu et al. 1999), and mitochondrial permeability transition pore inhibitors (e.g., cyclosporin A and metformin) can block apoptosis in cortical neurons (El-Mir et al. 2008). In contrast to Bax, which resides primarily in the cytosol (Hsu et al. 1997), Bak is a constitutive integral mitochondrial membrane protein (Wang et al. 2001), even in cells not exposed to death stimuli, and can interact with other resident or translocated mitochondrial proteins to alter its death permissibility function. Because Bax and Bak are both involved causally in the mechanisms for apoptosis of immature and differentiated cortical neurons (Fig. 7), the absence of either one of these proteins could affect the operation of the other, possibly through the formation of heteroligomeric complexes (Nechushtan et al. 2001) or by interaction with the VDAC (Shimizu et al. 2000) or other mitochondrial permeability transition pore components (Bernardi et al. 2006). Our finding suggests that multidomain proapoptotic Bcl-2 family members do not have completely redundant functions in cortical neurons.

Puma and Noxa are Upregulated in Cortical Neurons during Apoptosis

BH3-only proapoptotic proteins can link DNA damage-induced p53 activation to mitochondria in non-neural cells (Jeffers et al. 2003), but this connection is not clear in neurons. We found that Puma and Noxa protein levels are elevated in cortical neurons undergoing DNA damage-induced apoptosis. Our Puma result is consistent with the upregulated Puma mRNA and protein in cytosine arabinoside-treated sympathetic ganglion neurons (Wyttenbach and Tolkovsky 2006) and in DIV6 postnatal cortical neuron cultures undergoing arsenite-induced apoptosis (Wong et al. 2005). Puma mRNA upregulation is also found in CPT-treated cerebellar granule neurons (Cregan et al. 2004). Increased Noxa mRNA expression occurs in DIV6 postnatal cortical neurons undergoing arsenite-induced apoptosis (Wong et al. 2005). Of greater conceptual importance is the observation made here that undifferentiated and differentiated neurons have distinct temporal profiles for Puma and Noxa protein upregulation; thus, the upregulation of some p53 target genes or the mobilization of their gene products is different in cortical neurons undergoing apoptosis depending on maturation state.

Immature and Mature Cortical Neuron Use Caspase-3 for Apoptosis

Our study shows that caspase-3 has a major participatory role in the mechanisms of DNA damage-induced apoptosis in cortical neurons that are undifferentiated and well-differentiated. Most related studies on cortical neurons have been done on immature, undifferentiated DIV1–4 neurons and have not identified definitively the roles of caspases in CPT-induced apoptosis. Protection against CPT-induced apoptosis has been seen with 100 μM caspase-3 inhibitor in rat embryonic cortical neurons at DIV1 (Stefanis et al. 1999) and mouse telencephalic neuron cultures at DIV4 (Johnson et al. 1999). Caspase inhibition protected partially against and delayed CPT-induced apoptosis in mouse embryonic cortical neurons at DIV2 (Keramaris et al. 2000); yet, other experiments have failed to block CPT-induced apoptosis of DIV2 neurons with caspase inhibitor (Park et al. 1998), and neuronal death was only delayed by 24 h in neurons without caspase-3 (Keramaris et al. 2000). We found previously a near complete block of CPT-induced apoptosis with a reversible peptide inhibitor of caspase-3 in DIV5 cortical neurons, but with differentiated cortical neurons the peptide inhibitor was much less effective, despite the CPT-induced presence of cleaved caspase-3 at both in vitro ages (Lesuisse and Martin 2002b). Here we show that a novel small-molecule, non-peptide caspase-3 inhibitor blocks significantly CPT-induced apoptosis in immature neurons as well as differentiated cortical neurons in vitro. This finding highlights a difference in neuroprotective actions of small-molecule versus peptide inhibitors of caspases. More importantly, this finding on caspase-3 demonstrates that the molecular mechanisms of DNA damage-induced cell death in cortical neurons converge downstream in the apoptotic pathway independent of neuron differentiation state.

Conclusions and Relevance to Human Cerebral Cortex

The execution of apoptosis in neurons of cerebral cortex triggered by DNA damage is multifactorial involving at least 4 molecular networks (ATM/c-Abl protein kinases, p53, Bcl-2 multidoman and BH3-only family members, and caspases). Another level of complexity is differential molecular signaling in response to DNA damage depending upon neuronal differentiation state or age. The activation of p53 and coinciding neuronal apoptosis in cortical neurons with DNA damage is not merely an in vitro system-specific process, because similar molecular and morphological events occur in cerebral cortex after CPT treatment in mice.

DNA damage-induced, p53-mediated cell death possibly contributes to cortical neuron degeneration in human disorders (Martin 2001; Martin et al. 2005). In age-related diseases, if cortical neurons accumulate selectively DNA strand breaks as part of the mechanistically relevant pathobiology (Mullaart et al. 1990), then why is the neurodegeneration apparently slow, in light of evidence on mouse neurons showing that when DNA strand breaks accumulate, the p53-cell death response is rapid and robust? There is likely a balance between steady-state DNA strand break accumulation and DNA repair capacity. Inefficiency in DNA repair or enhanced DNA strand break formation could be acquired slowly over time (aging) in neurons with the amount of DNA damage accumulating initially at subthreshold levels for engaging cell death mechanisms. DNA damage could accumulate asynchronously in subsets of disease-vulnerable postmitotic neurons during aging that are eliminated individually slowly over time through p53-mediated mechanisms. Another possibility is that p53 activation can be independent of DNA damage (Ohyagi et al. 2005). Neocortical neurons need to be protected against age- and injury-related degeneration because endogenous postnatal genesis of these neurons in primates is rare (Rakic 2002; Breunig et al. 2007). Thus, strategies for neuroprotection in cerebral cortex will need to be age appropriate due to differences in cell death mechanisms in neurons at different stages of maturity (Fig. 7).

Funding

U.S. Public Health Service, National Institutes of Health, National Institute of Neurological Disorders, and Stroke (NS052098 and NS034100); and National Institute on Aging (AG016282).

Notes

We are grateful for the expert technical assistance of Ann Price and Yan Pan. L.J.M. thanks Dr Christian Lesuisse for his inspirational work with this neuronal culture model and Drs John Jeffers and Gerard Zambetti (St Jude Children's Research Hospital) for providing *puma* null mice. L.J.M. dedicates this manuscript to the memory of his father, Joseph G. Martin (born, June 10, 1926; died, December 21, 2007). *Conflict of Interest*: None declared.

Address correspondence to Dr Lee J. Martin, Johns Hopkins University School of Medicine, Department of Pathology, 558 Ross Building, 720 Rutland Avenue, Baltimore, MD 21205-2196, USA. Email: martinl@jhmi.edu.

References

Adamec E, Vonsattel JP, Nixon RA. 1999. DNA strand breaks in Alzheimer's disease. Brain Res. 849:67–77.

Bendixen C, Thomsen B, Alsner J, Westergaard O. 1990. Camptothecin-stabilized topoisomerase I-DNA adducts cause premature termination of transcription. Biochemistry. 29:5613–5619.

Bernardi P, Krauskopf A, Basso E, Petronilli V, Blalchy-Dyson E, Di Lisa F, Forte MA. 2006. The mitochondrial permeability transition from in vitro artifact to disease target. FEBS J. 273:2077–2099.

Blasina A, Price BD, Turenne GA, McGowan CH. 1999. Caffeine inhibits the checkpoint kinase ATM. Curr Biol. 9:1135–1138.

Bombrun A, Gerber P, Casi G, Terradillos O, Antonsson B, Halazy S. 2003. 3,6-Dibromocarbazole piperazine derivatives of 2-propanol as first inhibitors of cytochrome c release via bax channel modulation. J Med Chem. 46:4365–4368.

Breunig JJ, Arellano JI, Macklis JD, Rakic P. 2007. Everything that glitters isn't gold: a critical review of postnatal neural precursor analysis. Cell Stem Cell. 1:612–627.

Chao C, Saito S, Anderson Cw, Appella E, Xu Y. 2000. Phosphorylation of murine p53 at Ser-18 regulates the p53 response to DNA damage. Proc Natl Acad Sci USA. 97:11936–11941.

Chen J, Jin K, Chen M, Pei W, Kawaguchi K, Greenberg DA, Simon RP. 1997. Early detection of DNA strand breaks in the brain after transient focal ischemia: implications for the role of DNA damage in apoptosis and neuronal cell death. J Neurochem. 69:232–245.

Chen Y-H, Zhang Y-H, Zhang H-J, Liu D-Z, Gu M, Li J-Y, Wu F, Zhu X-Z, Li J, Nan F-J. 2006. Design, synthesis, and biological evaluation of isoquinoline-1,3,4,-trione derivative as potent caspase-3 inhibitors. J Med Chem. 49:1613–1623.

Chipuk JE, Kuwana T, Bouchier-Hayes L, Droin NM, Newmeyer DD, Schuler M, Green DR. 2004. Direct activation of Bax by p53 mediates mitochondrial membrane permeabilization and apoptosis. Science. 303:1010–1014.

Clark RSB, Chen M, Kochanek PM, Watkins SC, Jin KL, Draviam R, Nathaniel PD, Pinto R, Marion DW, Graham SH. 2001. Detection of single- and double-strand DNA breaks after traumatic brain injury in rats: comparison of in situ labeling techniques using DNA polymerase I, the Klenow fragment of DNA polymerase I, and terminal deoxynucleotidyl transferase. J Neurotrauma. 18:675–689.

Cregan SP, Arbour NA, MacLaurin JG, Callaghan SM, Fortin A, Cheung ECC, Guberman DS, Park DS, Slack RS. 2004. p53 activation domain 1 is essential fro PUMA upregulation and p53-mediated neuronal cell death. J Neurosci. 24:10003–10012.

Cregan SP, MacLaurin JG, Craig CG, Robertson GS, Nicholson DW, Park DS, Slack RS. 1999. Bax-dependent caspase-3 activation is a key determinant in p53-induced apoptosis in neurons. J Neurosci. 19:7860–7869.

De la Monte SM, Sohn YK, Wands JR. 1997. Correlates of p53- and Fas (CD95)-mediated apoptosis in Alzheimer's disease. J Neurol Sci. 152:73–83.

D'Sa-Eipper C, Leonard JR, Putcha G, Zheng TS, Flavell RA, Rakic P, Kuida K, Roth KA. 2001. DNA damage-induced neural precursor cell apoptosis requires p53 and caspase 9 but neither Bax nor caspase 3. Development. 126:137–146.

Dumaz N, Milne DM, Jardine LJ, Meek DW. 2001. Critical roles for the serine 20, but not the serine 15, phosphorylation site and for the polyproline domain in regulating p53 turnover. Biochem J. 359:469–464.

El-Mir M-Y, Detaille D, R-Villanueva G, Delgado-esteban M, Guigas B, Atrtia S, Fontaine E, Almeida A, Leverve X. 2008. Neuroprotective role of antidiabetic drug metformin against apoptotic cell death in primary cortical neurons. J Mol Neurosci. 34:77–87.

Endokido Y, Araki T, Tanaka K, Aizawa S, Hatanaka H. 1996. Involvement of p53 in DNA strand break-induced apoptosis in postmitotic CNS neurons. Eur J Neurosci. 8:1812–1821.

Figueroa-Masot XA, Hetman M, Higgins MJ, Kokot N, Xia Z. 2001. Taxol induces apoptosis in cortical neurons by a mechanism independent of Bcl-2 phosphorylation. J Neurosci. 21:46-57–46-67.

Giaccia AJ, Kastan MB. 1998. The complexity of p53 modulation: emerging patterns from divergent signals. Genes Dev. 12: 2973–2983.

Gomez-Isla T, Hollister R, West H, Mui S, Growdon JH, Petersen RC, Parisi JE, Hyman BT. 1997. Neuronal loss correlates with but exceeds neurofibrillary tangles in Alzheimer's disease. Ann Neurol. 41:17–24.

Hedreen JC, Peyser CE, Folstein SE, Ross CA. 1991. Neuronal loss in layers V and VI of cerebral cortex in Huntington's disease. Neurosci Lett. 133:257–261.

Hetz C, Vite P-A, Bombrun A, Rostovtseva TK, Montessuit S, Hiver A, Schwarz MK, Chruch DJ, Kosrmeyer SJ, Martinou J-C, et al. 2005. Bax channel inhibitors prevent mitochondrion-mediated apoptosis and protect neurons in a model of global brain ischemia. J Biol Chem. 280:42960–42970.

Hickson I, Zhao Y, Richardson CJ, Green SJ, Martin NMB, Orr AI, Reaper PM, Jackson SP, Curtin NJ, Smith GCM. 2004. Identification and characterization of a novel and specific inhibitor of the ataxia-telangiectasia mutated kinase ATM. Cancer Res. 64:9152–9159.

Holinger EP, Chittenden T, Lutz RJ. 1999. Bak BH3 peptides antagonize Bcl-xL function and induce apoptosis through cytochrome c-independent activation of caspases. J Biol Chem. 274:13298–13304.

Hou ST, MacManus JP. 2002. Molecular mechanisms of cerebral ischemia-induced neuronal death. Intl Rev Cytol. 221:93–148.

Hsu YT, Wotter KG, Youle RJ. 1997. Cytosol-to-membrane redistribution of Bax and Bcl-X(L) during apoptosis. Proc. Natl. Acad. Sci. USA. 94:3668–3672.

Huang D, Shenoy A, Cui J, Huang W, Liu PK. 2000. In situ detection of AP sites and DNA strand breaks bearing 3′-phosphate termini in ischemic mouse brain. FASEB J. 14:407–417.

Igata E, Inoue T, Ohtani-Fujita N, Sowa Y, Tsujimoto Y, Sakai T. 1999. Molecular cloning and functional analysis of the murine bax gene promoter. Gene. 238:407–415.

Jeffers JR, Parganas E, Lee Y, Yang C, Wang J, Brennan J, MacLean KH, Han J, Chittenden T, Ihle JN, et al. 2003. Puma is an essential mediator of p53-dependent and –independent apoptotic pathways. Cancer Cell. 4:321–328.

Johnson MD, Kinoshita Y, Xiang H, Ghatan S, Morrison RS. 1999. Contribution of p53-dependent caspase activation to neuronal cell death declines with neuronal maturation. J Neurosci. 19:2996–3006.

Johnston MV. 2004. Clinical disorders of brain plasticity. Brain Dev. 26:73–80.

Kannan K, Amariglio N, Rechavi G, Jakob-Hirsch J, Kela I, Kaminski N, Getz G, Domany E, Givol D. 2001. DNA microarrays identification of primary and secondary target genes regulated by p53. Oncogene. 20:2225–2234.

Kastan MB, Lim D-S. 2000. The many substrates and functions of ATM. Nat Mol Cell Biol. 1:179–186.

Keramaris E, Hirao A, Slack RS, Mak TW, Park DS. 2003. Ataxia telangiectasia-mutated protein can regulate p53 and neuronal death independent of chk2 in response to DNA damage. J Biol Chem. 278:37782–37789.

Keramaris E, Stefanis L, MacLaurin J, Harada N, Takaku K, Ishikawa T-O, Taketa MM, Robertson GS, Nicholson DW, Slack RS, et al. 2000. Involvement of caspase 3 in apoptotic death of cortical neurons evoked by DNA damage. Mol Cell Neurosci. 15:368–379.

Kharbanda S, Yuan Z-M, Weichselbaum R, Kufe D. 1998. Determination of cell fate by c-Abl activation in response to DNA damage. Oncogene. 17:3309–3318.

Kindzelskii AL, Petty HR. 1999. Ultrasensitive detection of hydrogen peroxide-mediated DNA damage after alkaline single cell gel electrophoresis using occultation microscopy and TUNEL labeling. Mutat Res. 426:11–22.

Komarov PG, Komarova EA, Kondratov RV, Christov-Teselkov K, Coon JS, Chernov MV, Gudkov AV. 1999. A chemical inhibitor of p53 that protects mice from the side effects of cancer therapy. Science. 285:1733–1737.

Kuan C-Y, Schoemer AJ, Lu A, Burns KA, Weng W-L, Williams MT, Strauss KI, Vorhees CV, Flavell RA, Davis RJ, et al. 2004. Hypoxia-ischemia induces DNA synthesis without cell proliferation in dying neurons in adult rodent brain. J Neurosci. 24:10763–10722.

Lee Y, Chong MJ, McKinnon PJ. 2001. Ataxia telangiectasia mutated-dependent apoptosis after genotoxic stress in the developing nervous system is determined by cellular differentiation status. J Neurosci. 21:6687–6693.

Lesuisse C, Martin LJ. 2002a. Long-term culture of mouse cortical neurons as a model for neuronal development, aging, and death. J Neurobiol. 51:9–23.

Lesuisse C, Martin LJ. 2002b. Immature and mature cortical neurons engage different apoptotic mechanisms involving caspase-3 and the MAP kinase pathway. J Cereb Blood Flow Metab. 22:935–950.

Lindahl T. 1993. Instability and decay of the primary structure of DNA. Nature. 362:709–715.

MacDonald V, Halliday GM. 2002. Selective loss of pyramidal neurons in the pre-supplementary motor cortex in Parkinson's disease. Mov Disord. 17:1166–1173.

Macleod MR, Ramage LE, McGregor A, Seckl JR. 2003. Reduced NMDA-induced apoptosis in neurons lacking ataxia telangiectasia mutated protein. NeuroReport. 14:215–217.

Martin LJ. 2000. p53 is abnormally elevated and active in the CNS of patients with amyotrophic lateral sclerosis. Neurobiol Dis. 7:613–622.

Martin LJ. 2001. Neuronal cell death in nervous system development, disease, and injury. Int J Mol Med. 7:455–478.

Martin LJ. 2008. Forthcoming. Mechanisms of neurodegeneration and therapeutics in animal models of hypoxic-ischemic encephalopathy. In: Stevenson DK, Benitz WE, Sunshine P, editors. Fetal and neonatal brain brain injury. 4th ed. Cambridge: Cambridge University Press.

Martin LJ, Al-Abdulla NA, Brambrink AM, Kirsch JR, Sieber FE, Portera-Cailliau C. 1998. Neurodegeneration in excitotoxicity, global cerebral ischemia, and target deprivation: a perspective on the contributions of apoptosis and necrosis. Brain Res Bull. 46:281–309.

Martin LJ, Liu Z. 2002. DNA damage profiling in motor neurons: a single-cell analysis by comet assay. Neurochem Res. 27:1093–1104.

Martin LJ, Liu Z, Troncoso JC, Price DL. 2005. Neuronal cell death in human neurodegenerative diseases and their animal/cell models. In: Holcik M, LaCasse E, Korneluk R, MacKenzie A, editors. Apoptosis in health and disease. Cambridge: Cambridge University Press. p. 242–315.

Martin LJ, Price AC, McClendon KB, Al-Abdulla NA, Subramaniam JR, Wong PC, Liu Z. 2003. Early events of target deprivation/axotomy-induced neuronal apoptosis in vivo: oxidative stress, DNA damage, p53 phosphorylation and subcellular redistribution of death proteins. J Neurochem. 85:234–247.

McArthur JC, Brew BJ, Nath A. 2005. Neurological complications of HIV infection. Lancet Neurol. 4:543–555.

Miyashita T, Reed JC. 1995. Tumor suppressor p53 is a direct transcriptional activator of the human *bax* gene. Cell. 80:293–299.

Morris EJ, Geller HM. 1996. Induction of neuronal apoptosis by camptothecin, an inhibitor of DNA topoisomerase-I: evidence for cell cycle-independent toxicity. J Cell Biol. 134:757–770.

Morrison RS, Kinoshita Y Johnson MD, Guo W, Garden GA. 2003. p53-dependent cell death signaling in neurons. Neurochem Res. 28:15–27.

Mullaart E, Boerrigter METI, Ravid R, Swaab DF, Vijg J. 1990. Increased levels of DNA breaks in cerebral cortex of Alzheimer's disease patients. Neurobiol Aging. 11:169–173.

Nakagawa K, Taya Y, Tamai K, Yamaizumi. 1999. Requirement of ATM in phosphorylation of the human p53 protein at serine 15 following DNA double-strand breaks. Mol Cell Biol. 19:2828–2834.

Nakajima M, kashiwagi K, Ohta J, Furkawa S, Hayashi K, Kawashima T, Hayashi Y. 1994. Etoposide induces programmed death in neurons cultured from the fetal rat central nervous system. Brain Res. 4:350–352.

Narasimhaiah R, Tuchman A, Lin SL, Naegele JR. 2005. Oxidative damage and defective DNA repair is linked to apoptosis of migrating neurons and progenitors during cerebral cortex development in Ku70-deficient mice. Cereb Cortex. 15:696–707.

Nechushtan A, Smith CL, Lamensdorf I, Yoon S-H, Youle RJ. 2001. Bax and Bak coalesce into novel mitochondria-associated clusters during apoptosis. J Cell Biol. 153:1265–1276.

Nieves-Neira W, Pommier Y. 1999. Apoptotic response to camptothecin and 7-hydroxystaurosporine (UCN-01) in the 8 human breast cancer cell lines of the NCI anticancer drug screen: multifactorial relationships with topoisomerase I, protein kinase, Bcl-2, p53, MDM-2 and caspase pathways. Int J Cancer. 82:396–404.

Nihei K, McKee AC, Kowall NW. 1993. Pattern of neuronal degeneration in motor cortex of amyotrophic lateral sclerosis patients. Acta Neuropathol. 86:55–64.

Nitiss JL, Wang JC. 1996. Mechanisms of cell killing by drugs that trap covalent complexes between DNA topoisomerases and DNA. Mol Pharmacol. 50:1095–1102.

Northington FJ, Zelaya ME, O'Riordan DP, Blomgren K, Flock DL, Hagberg H, Ferriero DM, Martin LJ. 2007. Failure to complete apoptosis following neonatal hypoxia-ischemia manifests as "continuum" phenotype of cell death and occurs with multiple manifestations of mitochondrial dysfunction in rodent forebrain. Neuroscience. 149:822–833.

Ohyagi Y, Asahara H, Chui D-H, Tsuruta Y, Sakae N, Miyoshi K, Yamada T, Kikuchi H, Taniwaki T, Murai H, et al. 2005. Intracellular Aβ activates p53 promoter: a pathway to neurodegeneration in Alzheimer's disease. FASEB J. 19:225–257.

Park DS, Morris EJ, Stefanis L, Troy CM, Shelanski ML, Geller HM, Greene LA. 1998. Multiple pathways of neuronal death induced by DNA-damaging agents, NGF deprivation, and oxidative stress. J Neurosci. 18:830–840.

Pohl U, Wagenknecht B, Naumann U, Welleer M. 1999. p53 enhances Bak and CD95 expression in human malignant glioma cells but does not enhance CD95L-induced apoptosis. Cell Physiol Biochem. 9:29–37.

Portera-Cailliau C, Price DL, Martin LJ. 1997. Excitotoxic neuronal death in the immature brain is an apoptosis-necrosis morphological continuum. J Comp Neurol. 378:70–87.

Raina D, Mishra N, Kumar S, Kharbanda S, Saxena S, Kufe D. 2002. Inhibition of c-Abl with STI571 attenuates stress-activated protein kinase activation and apoptosis in the cellular response to 1-β-D-arabinofuranosylcytosine. Mol Pharmacol. 61:1489–1495.

Rakic P. 2002. Neurogenesis in adult primate neocortex: an evaluation of the evidence. Nat Rev Neurosci. 3:65–71.

Romero AA, Gross SR, Cheng KY, Goldsmith NK, Geller HM. 2003. An age-related increase in resistance to DNA damage-induced apoptotic cell death is associated with development of DNA repair. J Neurochem. 84:1275–1287.

Sawada M, Hayes P, Matsuyama S. 2003. Cytoprotective membrane-permeable peptides designed from Bax-binding domain of Ku70. Nat Cell Biol. 5:352–357.

Schmidt T, Korner K, Karsunky H, Korsmeyer S, Muller R, Moroy T. 1999. The activity of the murine Bax promoter is regulated by Sp1/3 and E-box binding protein but not by p53. Cell Death Differ. 6:873–882.

Shaikh AY, Martin LJ. 2002. DNA base-excision repair enzyme apurinic/apyrimidinic endonuclease/redox factor-1 is increased and competent in brain and spinal cord of individuals with amyotrophic lateral sclerosis. Neuromolecular Med. 2:47–60.

Shimizu S, Konishi A, Kodama T, Tsujimoto Y. 2000. BH4 domain of antiapoptotic Bcl-2 members closes voltage-dependent anion channel and inhibits apoptotic mitochondrial changes and cell death. Proc Natl Acad Sci USA. 97:3100–3105.

Shimizu S, Narita M, Tsujimoto Y. 1999. Bcl-2 family proteins regulate the release of apoptogenic cytochrome c by the mitochondrial VDAC. Nature. 399:483–487.

Slack RS, Belliveau DJ, Rosenberg M, Atwal J, Lochmuller H, Aloyz R, Haghighi A, Lach B, Seth P, Cooper E, et al. 1996. Adenovirus-mediated gene transfer of the tumor suppressor, p53, induces apoptosis in postmitotic neurons. J Cell Biol. 135:1085–1096.

Stefanis L, Park DS, Friedman WJ, Greene LA. 1999. Caspase-dependent and -independent death of camptothecin-treated embryonic cortical neurons. J Neurosci. 19:6235–6247.

Strom E, Sathe S, Kamarov PG, Chernova OB, Pavlovska I, Shyshynova I, Bosykh DA, Burdelya LG, Macklis RM, Skaliter R, et al. 2006. Small-molecule inhibitor of p53-binding to mitochondria protects mice from gamma radiation. Nat Chem Biol. 2:474–479.

Sze C-I, Troncoso JC, Kawas C, Mouton P, Price DL, Martin LJ. 1997. Loss of the presynaptic vesicle protein synaptophysin in hippocampus correlates with cognitive decline in Alzheimer disease. J Neuropathol Exp Neurol. 56:993–944.

Thornborrow EC, Patel S, Mastropietro AE, Schwartzfarb EM, Manfredi JJ. 2002. A conserved intronic response element mediates direct p53-dependent transcriptional activation of both the human and murine bax genes. Oncogene. 21:990–999.

Tice RR, Agurell E, Anderson D, Burlinson B, Hartmann A, Kobayashi H, Miyamae Y, Rojas E, Ryu J-C, Sasaki YF. 2000. Single cell gel/comet assay: guidelines for in vitro and in vivo genetic toxicology testing. Environ Mol Mutagen. 35:206–221.

Wang G-Q, Gastman BR, Wieckowski E, Goldstein LA, Gambotto A, Kim T-H, Fang B, Rabinovitz A, Yim XM, Rabinowich H. 2001. A role for mitochondrial Bak in apoptotic response to anticancer drugs. J Biol. Chem. 276:34307–34317.

Wong HK, Fricker M, Wyttenbach A, Villunger A, Michalak EM, Strasser A, Tolkovsky AM. 2005. Mutually exclusive subsets of BH3-only protein are activated by p53 and c-Jun N-terminal kinase/c-Jun signaling pathways during cortical neuron apoptosis induced by arsenite. Mol Cell Biol. 25:8732–8747.

Wyttenbach A, Tolkovsky AM. 2006. The BH3-only protein Puma is both necessary and sufficient for neuronal apoptosis induced by DNA damage in sympathetic neurons. J Neurochem. 96:1213–1226.

Xiang H, Hochman DW, Sava H, Fujwara T, Schwartzkroin PA, Morrison RS. 1996. Evidence for p53-mediated modulation of neuronal viability. J Neurosci. 16:6753–6765.

Xiang H, Kinoshita Y, Knudson CM, Korsmeyer SJ, Schwartzkroin PA, Morrison RS. 1998. Bax involvement in p53-mediated neuronal cell death. J Neurosci. 18:1363–1373.

Yang Y, Geldmacher DS, Herrup K. 2001. DNA replication precedes neuronal cell death in Alzheimer's disease. J Neurosci. 21:2661–2668.

Zhang X, Chen Y, Jenkins LW, Kochanek PM, Clark RS. 2005. Bench-to-bedside review: Apoptosis/programmed cell death triggered by traumatic brain injury. Crit Care. 9:66–75.

Zhang Y, McLaughlin R, Goodyer C, LeBlanc A. 2002. Selective cytotoxicity of intracellular amyloid β peptide$_{1-42}$ through p53 and Bax in cultured primary human neurons. J Cell Biol. 156:519–529.